2013•2014
FACULTEIT GENEESKUNDE EN LEVENSWETENSCHAPPEN
master in de biomedische wetenschappen

Masterproef

Gender-related effects of advanced glycation end products on cardiac and renal function

Promotor :
Prof. dr. Virginie BITO

Copromotor :
dr. Quirine SWENNEN

Tugçe Arslan

Proefschrift ingediend tot het behalen van de graad van master in de biomedische wetenschappen

2013•2014
FACULTEIT GENEESKUNDE EN LEVENSWETENSCHAPPEN
master in de biomedische wetenschappen

Masterproef

Gender-related effects of advanced glycation end products on cardiac and renal function

Promotor :
Prof. dr. Virginie BITO

Copromotor :
dr. Quirine SWENNEN

Tugçe Arslan

Proefschrift ingediend tot het behalen van de graad van master in de biomedische wetenschappen

universiteit hasselt | Maastricht University

Acknowledgements

I dedicate this work to my father, who always supported me in this though life. I know he is still watching over me and guiding me from the other side. All the achievements that I will make for the rest of my life will be dedicated to him and to my family. To my mother for always pushing me to be the best I could be and always supporting me, whatever decision that I took. You are the best mother in this world I can ever imagine. And not to forget, to my little friend, my brother. Your being is enough to keep me going on.

To my supervisor Virginie Bito for allowing me to be a member of her team and being always helpful. With her deep knowledge in science and her humanity, she added so many things to my scientific knowledge and personal thinking. As you always say Virginie, thanks a lot! I'm grateful to my co-promotor Quirine Swennen for all her helps and contributions throughout my internship.

I deeply appreciate the help that my mentors, Dorien Deluyker and Vesselina Ferferieva, have provided me. Big thanks for your guidance trough the tangled web of experiments and articles, and your encouragement throughout the entire process.

I would also like to thank my second examiner, Leen De Ryck, for all her contributing advices. Last, but not least, big thanks to Jasmina and Joris for their help and support during the experiments.

TABLE OF CONTENTS

LIST OF FIGURES AND TABLES

LIST OF ABBREVIATIONS

AGEs	advanced glycation end products
AWT	anterior wall thickness
BSA	bovine serum albumin
CHF	chronic heart failure
CML	N(epsilon)-(carboxymethyl)lysine
CRS	cardio-renal syndrome
CO	cardiac output
ECL	enhanced chemiluminescence
EDV	end diastolic volume
EF	ejection fraction
ESV	end systolic volume
ELISA	enzyme-linked immunosorbent assay
FS	fractional shortening
HEPES	4-(2-hydroxyethyl)-1-piperazineethanesulfonic acid
HRP	horseradish peroxidase
i.p	intraperitoneal
KIM-1	kidney injury molecule-1
LV	left ventricle
NO	nitric oxide
PBS	phosphate buffered saline
PFA	paraformaldehyde
PVDF	polyvinylidene fluoride
PWT	posterior wall thickness
RAGE	receptor for advanced glycation end products
ROS	reactive oxygen species
SDS-PAGE	sodium dodecyl sulphate polyacrylamide gel
sRAGE	soluble RAGE
SV	stroke volume
TBS-T	tris-buffered saline with tween 20
TNF-α	tumor necrosis factor-alpha
TGF-β	transforming growth factor-beta
VEGF	vascular endothelial growth factor

NEDERLANDSE SAMENVATTING

AGEs zijn eiwitten of vetten die *in vivo* versuikerd worden. Enerzijds is er steeds meer bewijs dat AGEs mogelijk ook betrokken zijn in de ontwikkeling en vooruitgang van hart- en nierfalen. Anderzijds is het bekend dat vrouwen over het algemeen minder gevoelig zijn aan cardiovasculaire aandoeningen. De huidige studie had als doel om het effect van AGEs op de hart- en nierfunctie en om de geslachtsverschillen in hart- en nierfunctie te bestuderen als gevolg van verhoogde AGEs in het lichaam. Mannelijke en vrouwelijke Sprague-Dawley ratten werden dagelijks i.p geïnjecteerd met AGEs (20 mg/kg) of BSA met eenzelfde concentratie gedurende 6 weken. Urinestalen werden voor-en na 6 weken injecties verzameld. Echocardiografie metingen bij de start van de studie en na 6 weken behandeling werd uitgevoerd om de hartfunctie te volgen. Na 6 weken werden de dieren opgeofferd en werd het hart- en nierweefsel verzameld voor *ex vivo* onderzoek, met aandacht voor AGEs, receptor voor AGEs (RAGE) en fibrose. Injecties van AGEs gedurende 6 weken leidden tot hart dysfunctie. Echocardiografie toonde significante morfologische veranderingen van hartspierweefsel in beide geslachten. Hypertrofie werd bevestigd met een verhoogd hart gewicht-tibia lengteverhouding in beide geslachten. Totaal collageen was hoger in AGE-BSA geïnjecteerde dieren, waarbij het totaal collageen hoger was bij mannen dan bij vrouwen. AGE-BSA geïnjecteerde ratten vertoonden een stijgende trend in RAGE expressie in hartweefsel vergeleken met controlegroepen. Urine analyse toonde veranderingen in elektrolyt concentraties van AGE-BSA behandelde mannelijke dieren en fibrose was uitgesproken in de cortex. Deze studie toont aan dat AGE-BSA injecties aanleiding geven tot fibrose in zowel het hartweefsel als nierweefsel. Mannelijke ratten vertonen meer uitgesproken fibrose dan de vrouwtjes wat de duidelijke verslechtering in hartfunctie *in vivo* deels verklaart.

ABSTRACT

Advanced glycation end products (AGEs) are considered to have a possible role on the development and progression of cardiovascular and renal failure. However, there seems to be gender differences in the incidence of these diseases. The present study aimed to assess the gender-related differences on the cardiac and renal function outcome due to increased circulating AGEs levels. Male and female Sprague-Dawley rats were injected daily with BSA-modified AGEs (AGEs, 20 mg/kg, i.p) or control (BSA) for 6 weeks. Urine samples were collected at baseline and 6 weeks after treatment. Echocardiography at baseline and after 6 weeks was used to assess cardiac function. After 6 weeks, heart and kidney tissue was collected for various examinations *ex vivo* (immohistochemistry, western blotting analysis), focusing on the receptor for AGEs (RAGE), AGEs and fibrosis. Injections of AGEs for 6 weeks led to cardiac dysfunction. Echocardiography showed significant morphological changes of myocardial tissue in both genders. Hypertrophy was confirmed with an increased heart weight-to-tibia length ratio in both genders. In addition, LV volumes (end diastolic-end systolic) significantly increased compared to baseline in both genders, but this increase was less pronounced in females compared to males. Total collagen was higher in AGE-BSA injected animals, with a substantial increase in males compared to females. Moreover, AGE-BSA treated rats showed an increasing trend in RAGE expression in heart tissue compared to control groups. Urine analysis showed changes in electrolyte concentrations of AGE-BSA treated males and fibrosis was pronounced the cortex. In conclusion, daily AGEs injections lead to cardiac dysfunction in male and female rats. More pronounced extracellular remodeling (i.e. fibrosis) in males partially explain the worsening of cardiac dysfunction observed *in vivo*.

1 INTRODUCTION

1.1 CARDIO-RENAL SYNDROME

1.1.1 Pathophysiology

Heart performance and kidney function are closely interconnected physiologically and pathophysiologically. There is a growing evidence of kidney disease in individuals with heart disease and this has become a major public health concern since the mortality in these patients is increasing. The condition whereby acute or chronic dysfunction in one organ may induce dysfunction of the other organ is referred to as the cardio-renal syndrome (CRS) (1). The pathophysiology of CRS remains unclear but can be attributed to three main factors: neurohormonal and inflammatory activation, decreased renal perfusion due to low cardiac output and endothelial dysfunction (2, 3). Ultimately, these events may induce structural and functional damage in both heart and kidneys in a feedback loop leading to even more cardiac and renal damage.

1.1.2 Cardiac remodeling and heart failure progression

There is general acceptance that as heart disease progresses into heart failure, heart size increases and cardiac function deteriorates. Cardiac remodeling may occur after pressure-or volume overload, myocardial infarction or inflammatory heart muscle diseases. This process is characterized by ventricular hypertrophy, myocardial fibrosis, and lengthening of action potential (4). When the heart is not able to compensate for these changes, it may evolve into heart failure, resulting from extracellular matrix (ECM) remodeling, myocyte lengthening and impaired systolic and/or diastolic dysfunction (5, 6). Remarkably, some researchers observed gender-related differences in cardiac remodeling (7) that partially can explain why females are more protected against cardiac disorders.

1.1.3 Effect of gender on cardiovascular and renal dysfunction

Compared to their male counterparts, women are at less risk of heart disease (8), with a higher incidence of sudden death in men (9). Typically, women develop cardiovascular diseases 10-20 years later than men, but, if present at a younger age, this disease has a more malign clinical course in women (10). Nowadays, there is still insufficient knowledge concerning the effect of gender on cardiac and renal dysfunction in euglycaemic conditions

and the mechanisms behind it. Gender differences are frequently observed in the cardiac response after myocardial infarction (MI). In this regard, Cavasin *et al.* showed in a mouse model of MI that male mice had a higher rate of cardiac rupture associated with a higher infarct expansion index. Moreover, males had significantly poorer LV function, more prominent dilatation and significant myocyte hypertrophy compared to females (11). Furthermore, many studies have focused on the influence of gender on cardiac and renal diseases in hyperglycaemic conditions, such as in diabetes mellitus. Stenvinkel *et al.* suggested that female end stage renal disease patients were more protected against inflammation and that sex hormones may have important cardioprotective effects (12). Also, spontaneously hypertensive male rats exhibited higher AGEs and oxidative stress than females, partially explaining the higher vulnerability of males to renal pathology (13). In conclusion, these studies suggest that there are gender differences in cardiovascular and renal diseases in euglycaemic as well as in hyperglycaemic conditions.

1.2 ADVANCED GLYCATION END PRODUCTS

1.2.1 AGEs chemistry

A possible role has been found for the non-enzymatic modification of proteins or lipids by glucose, a process which is known as glycation, in many pathological processes, such as rheumatoid arthritis (14), atherosclerosis (15), diabetes (16) and many others. It has been well studied that glycation products undergo modification over time *in vivo*, referred to as AGEs. AGEs are mainly generated through the non-enzymatic glycation and oxidation of proteins and lipids in the Maillard reaction (17). AGEs accumulation in the body is a normal process with aging. The Maillard reaction starts when proteins or lipids in the body are exposed to high levels of glucose leading to the production of an unstable compound known as “Schiff base”. This reaction further proceeds into the formation of “Amadori” products, which are more stable. After weeks or months, the Amadori products undergo further structural changes such as dehydration, degradation and oxidation to finally stable AGEs (18). These reactions are shown in Fig. 1 (19).

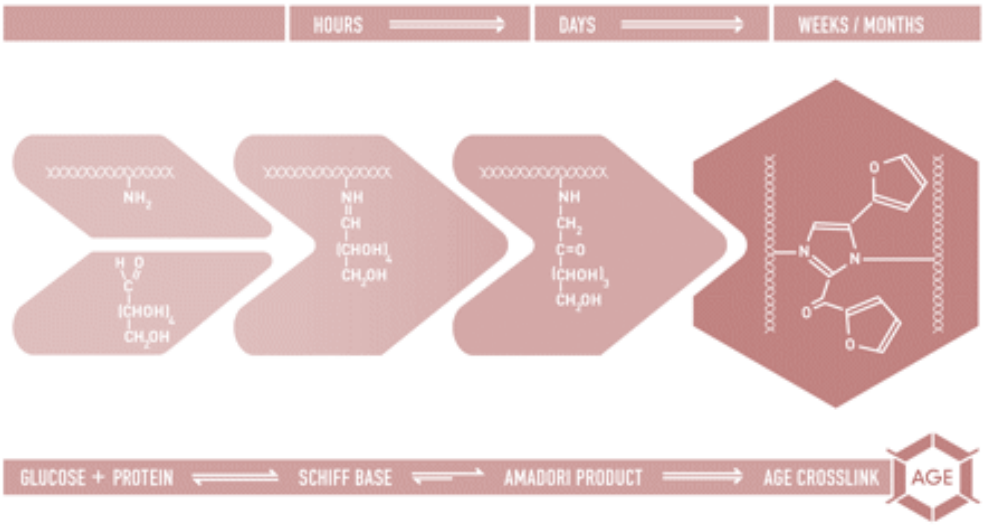

Figure 1: Maillard reaction. Schematic representation of the Maillard reaction; The first step is the reaction of a reducing sugar, such as glucose, with an amino acid. This reaction results further in a reaction product, called an Amadori product. The Amadori compounds can finally be rearranged into complex structures, called the AGEs.

1.2.2 AGEs structures

As mentioned before, production of AGEs involves the reaction of lysine with glucose and then either oxidation of the complex that leads to the formation of intermolecular cross-

links, such as the fluorescent pentosidine, or conversion of a Schiff base to the non-fluorescent N(epsilon)-(carboxymethyl)lysine (CML) (20, 21). Koyama *et al*. found that pentosidine, a well studied AGE structure, is involved in chronic heart failure (CHF) (22) while Schafer *et al.* showed that diastolic function correlated with levels of CML in diabetic rats (23). Interestingly, CML-AGEs are mainly related to severity and prognosis of CHF in patients (24) suggesting CML as a potential marker of CHF. However, this has to be further elucidated. Although pentosidine and CML are mainly described in research, AGEs comprises also many fluorescent and non-fluorescent AGEs structures as defined in Fig. S1 (Supplemental data).

1.2.2 Signalling pathways triggered by AGEs

There are 3 main mechanisms by which AGEs can potentially mediate their tissue effect regarding heart failure as shown in Fig. 2 (19). In a first mechanism, AGEs can cross-link proteins, such as collagen, in the ECM causing an increase in the ECM area leading to diastolic heart dysfunction with a disturbed LV filling. A second mechanism involves the interaction with the AGEs receptor; the interaction of AGEs with its best known receptor, RAGE, can cause fibrosis in the organs via the upregulation of TGF-β (25). The pro-inflammatory effect of AGE-RAGE interaction is mediated trough the activation of the NF-κB-pathway. Briefly, binding of AGEs by RAGE induces the generation of ROS and NADPH oxidase. The free radicals in turn activate a Ras-MAP-kinase pathway, which eventually leads to the activation of NF-κB. Activation and translocation of NF-κB to the nucleus result in the transcription of target genes (26). As a consequence, a couple of inflammatory cytokines and adhesion molecules are produced such as IL-6, TNF-α, VEGF, and intercellular adhesion molecule-1 (27, 28). In a third mechanism, AGE-RAGE interaction also influence calcium metabolism in cardiac myocytes. This interaction may lead to cross-linking intracellular proteins involved in myocyte functioning, such as sarcoendoplasmic reticulum calcium transport ATPase (SERCA), which may further evolve in heart failure.

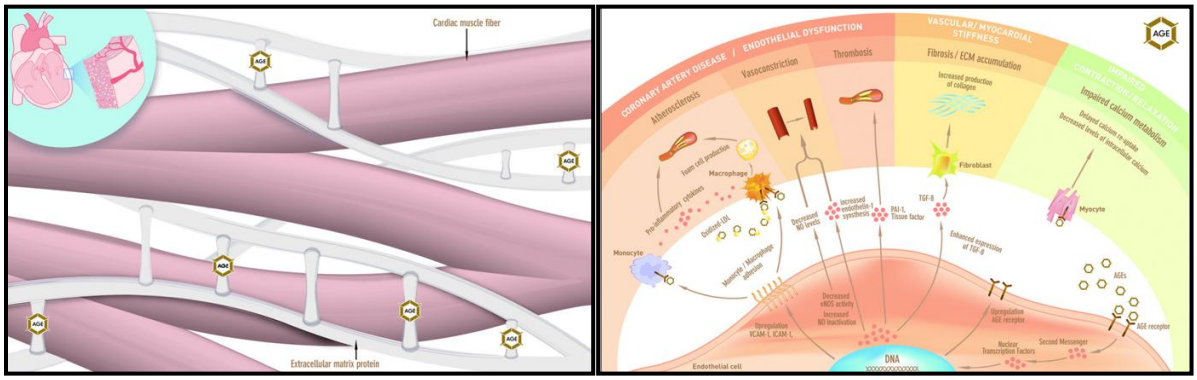

Figure 2: Signalling pathways triggered by AGEs. AGEs can cross-link proteins in ECM as shown in the left image. The right image inter alia shows the cellular responses to AGE-RAGE interaction in endothelial cells, and cardiac myocytes. AGE: adavanced glyaction end products; LDL: low-density lipoprotein; VCAM-1: vascular cell adhesion molecule-1; ICAM-1: intercellular adhesion molecule-1; PAI-1: plasminogen activator inhibitor-1; TGF-β: transforming growth factor-β; NO: nitric oxide; eNOS: endothelial nitric oxide synthesis; ECM: extracellular matrix.

1.2.3 Role of AGEs in heart and kidney failure

Increase in circulating AGEs has been shown to induce diastolic dysfunction in diabetic patients suffering from cardiomyopathy or nephropathy (29, 30). However, the involvement of AGEs does not seem to be limited to diabetes mellitus. Recently, it has been found that AGEs accumulates in patients with renal failure and heart failure (31, 32). The accumulation of AGEs in the kidney can be explained by the failing mechanism to clear excessive AGEs and enhanced oxidative stress causing increased formation of AGEs (33). However, the exact role of AGEs in cardiac and renal failure and the underlying mechanisms are still unrevealed.

1.3 RECEPTOR FOR ADVANCED GLYCATION END PRODUCTS

1.3.1 RAGE structure and isoforms

RAGE belongs to the immunoglobulin superfamily, and the protein consists of a V-type immunoglobulin-like domain, an N-terminal signal peptide, a single transmembrane domain, two tandem C-type immunoglobulin-like domains and a short C-terminal intracellular cytoplasmic tail (34). The V-domain is the binding site for AGEs (35), although other domains also play a role in diverse ligand binding (36). RAGE has a molecular weight of 45-55 kDa, which can be variable depending on differential glycosylation states (34).

Besides full-length RAGE, numerous isoforms of the receptor have been described as shown in Fig. 3 (34). The first described structure is the N-truncated isoform expressed on the cell

surface and this isoform is unable to interact with ligands because of lacking of the V-domain. Moreover, dominant negative-RAGE (DN-RAGE) misses the cytosolic domain, which results in no signal transduction, though it can bind to ligands. Soluble RAGE (sRAGE) is produced either by proteolytic cleavage of the full-length RAGE, called cleaved RAGE (cRAGE) or by alternative mRNA splicing, called the endogenous secretory RAGE (esRAGE). The sRAGE levels have been found to be elevated in coronary artery diseases, as well as in patients with heart failure (37, 38). sRAGE is able to circulate out of the cell and act as a scavenger by preventing ligands from binding to RAGE.

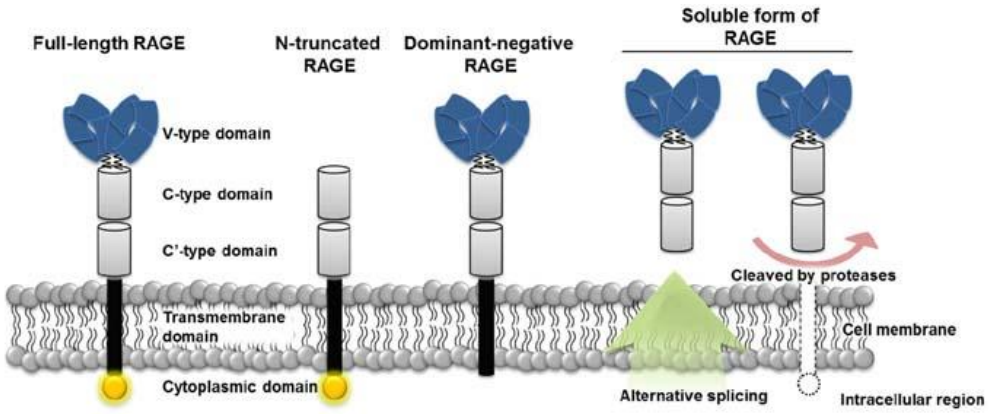

Figure 3: Structures of RAGE and its isoforms. Ligands bind to the V-domain of RAGE and transduce signals through the cytoplasmic domain. RAGE has three isoforms, called N-truncated, dominant-negative and soluble RAGE, generated either by alternative splicing or by the action of membrane-associated proteases. V: variable domain; C: constant domain.

1.3.2 RAGE expression in heart and kidney failure

The receptor is expressed in a wide range of tissues, such as liver, brain, kidney, heart and vasculature, and in diverse cell-types, including neurons, smooth muscle cells, endothelial cells, macrophages and cardiac myocytes (39). Elevated expression of RAGE has been demonstrated in endothelial cells in renal disease (40), as well as in cardiovascular tissue in diabetic rats (41). Increased levels of AGEs in the kidney and serum have been correlated with enhanced expression of AGEs receptors in mesangial cells (42). This indicates that the level of RAGE expression is regulated by the presence of its ligands.

1.3.3 The potential protective mechanism of sRAGE against heart and kidney dysfunction

sRAGE, which is composed of the extracellular domains but lacks the transmembrane and cytosolic domains, is produced by both proteolytic cleavage of RAGE and alternative mRNA splicing (43, 44). While membrane-bound RAGE promotes NF-κB (45) and ROS (46) signalling, sRAGE works as a capture mechanism of RAGE activating ligands, as shown by some researchers (47). Administration of sRAGE to euglycaemic apolipoprotein E-null mice with established atherosclerosis suppressed progression (48). Furthermore, Falcone *et al.* showed that endogenously lower levels of sRAGE were associated with enhanced risk of coronary artery disease in human (49). Contradictory, it has been shown that persons suffering from renal insufficiency show higher levels of sRAGE, because of either more production of AGEs and/or less efficient clearance (50). Consequently, no conclusions can be drawn yet regarding the protective effect of sRAGE against heart and kidney failure and further studies are needed to understand the complete mechanisms behind it.

1.4 AIM OF THE THESIS AND SIGNIFICANCE OF THE STUDY

It is clear that there are gender-related differences in the outcome of cardiovascular and renal failure but mechanisms behind gender-related differences remain unclear. Several experimental and clinical studies support the view that AGEs might have a crucial role in the pathogenesis of CRS by contributing to its development and progression. Since the clinical outcome of patients suffering from both cardiac and renal failure is worse and women show a remarkable lower incidence for this event, the aim of this pilot study was to investigate whether (1) increase in AGEs levels leads to cardiac and renal dysfunction and (2) whether this is gender-related.

2 MATERIALS & METHODS

2.1 ANIMALS

All studies on male and female rats were performed with the approval of the Committee for Animal Experimentation, UHasselt. 3-month-old male and female Sprague- Dawley rats (n= 14) purchased from the Charles River (Netherlands) were used for this pilot study. All animals were fed standard pellet diet and had water at their disposal *ad libitum*. They were maintained in a controlled environmental condition of temperature, light and humidity. Rats were sacrificed after 6 weeks of injections.

2.2 PREPARATION AND IDENTIFICATION OF AGEs

AGEs were prepared by incubation of 7 mg/mL low-endotoxin BSA (Sigma-Aldrich®, Belgium) with 90 mM glycolaldehyde dimers (Sigma-Aldrich®, Belgium) at 37.1°C for 5 days. The control solution was prepared by incubation of 7 mg/mL BSA at 37.1°C for 5 days. The free sugar was removed with dialysis against PBS by means of Slide-A-Lyzer® Dialysis Cassette G2 (Thermo Scientific, Belgium). Next, the samples were highly concentrated with means of Amicon Ultra centrifugal filter units obtained from Merck Millipore (Belgium). The protein concentration of both control and AGE-BSA samples was determined by means of the Pierce™ BCA Protein Assay Kit (Thermo Scientific, Belgium). The formation of AGEs was validated by performing a fluorescence measurement including the positive control purchased from Merck Millipore (Belgium). The fluorescence spectra were recorded on a Fluostar Optima spectrometer (BMG labtech, Germany) at room temperature. Gain adjustment was performed for each well. The excitation wavelength was set to 370 nm, and the signal intensity was measured at the emission maximum of 460 nm and expressed in arbitrary units (A.U.). In addition, coomassie staining was performed to visualize the protein pattern of the AGE-BSA and control samples.

2.3 EXPERIMENTAL PROTOCOL

Rats underwent daily i.p injections of 20 mg/kg BSA-modified AGEs or control (BSA) for 6 weeks. This concentration is based on previous research and moreover, diseased humans show AGEs range between 20-40 mg/kg. Male (n=4) and female (n=5) rats were subjected to the AGEs treatment. Control groups of males (n=2) and females (n=2) were included that were injected with dialysed BSA. Blood samples were obtained from the tail artery of rats

with a two-week interval. Echocardiography at baseline and after 6 weeks was used to assess cardiac function. Additionally, urine was sampled at baseline and 6 weeks of treatment. After 6 weeks, animals were sacrificed and heart/kidney tissue was sampled for *ex vivo* examinations (immunohistochemistry, western blot analysis), focusing on AGEs, RAGE and fibrosis.

2.3.1 Metabolic cages were used for urine sampling

In order to sample baseline urine and urine after 6 weeks of injections, 6 female and 6 male rats, each group consisting of 2 controls and 4 treated animals, were placed in metabolic cages as shown in Fig. 4. The body weight of the animals, food and water were monitored before and 24h after housing the animals in the metabolic cage. The urine samples were centrifuged and aliquots were frozen at -20°C.

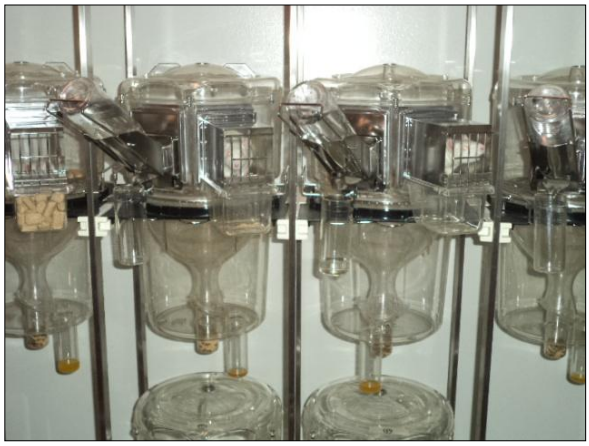

Figure 4: Picture of the metabolic cages. The animals were housed on metabolic cages for 24h urine collection.

2.3.2 Quantification of biomarkers

Blood and urine samples were obtained at regularly periods as mentioned before. Briefly, rats were anesthetized with isoflurane (2-4% mg/kg) in order to sample blood. Both serum and plasma blood samples were obtained from the tail artery of the animals. Urine samples were collected as mentioned before. Serum and plasma aliquots were frozen at -80°C. Urine was stored frozen at -20°C.

Kidney damage was evaluated in urine by measuring KIM-1, which is an early indicator for proximal tubule injury. The Duoset ELISA kit was obtained from R&D Systems^{TM} (UK). Cardiac function was evaluated by measuring CML concentration in serum. The ELISA kit was

obtained from the company My BioSource (Belgium). The protocol is summarized for KIM-1 and CML.

Briefly, the 96-well plate was pre-coated with anti-rat KIM-1 or anti-rat CML antibody. Urine previously stored at -20°C was plated together with the control and the standard samples for KIM-1 measurement. Serum was centrifuged at 2000 rpm for 20 min for CML measurements. The supernatant was collected and was set on the plate together with the control and the standard samples. All samples were mixed with a sample diluents buffer and incubated for 30 min at 37°C. Next, the plates were washed five times with washing buffer. Then, the HRP conjugated anti-KIM-1 antibody or anti-CML antibody was added to the wells and the plates were again incubated for 30 min at 37°C. After a second wash, TMB chromogenic reagent was added to each well for CML and the plates were incubated at 37°C for 15 min. KIM-1 was detected by adding substrate solution, followed by 20 min incubation. Next, the reaction was stopped by adding a stop solution and the O.D. absorbance at 450 nm was read in a microplate reader. In addition, a second wavelength of 540 nm was used to correct for KIM-1 ELISA.

The absorbance for each sample was corrected with the zero well. The rat KIM-1 and rat CML concentration of the samples was interpolated from the standard curve.

2.3.3 Echocardiography measurements

Echocardiography in additional to the measurements of biomarkers indicating organ dysfunction was used to calculate cardiac function. The echocardiograms were performed and analyzed by a specialized team member. Each animal underwent echocardiography at baseline and after 6 weeks injections. Several parameters were evaluated in order to investigate the cardiac functioning. Briefly, echocardiography was performed with a 10-MHz linear transducer and a cardiovascular ultrasound system (VIVID e, GE Healthcare, USA). Long-axis and short-axis views were used to obtain M-mode and 2-dimensional images. Anterior wall thickness (AWTd) and posterior wall thickness (PWTd) were measured at short-axis midpapillary level. End diastolic volumes (EDV) and end systolic volumes were calculated from images obtained both from the long-axis and the short-axis. EDV was determined as $EDV= \pi (D_L x D^2)^3/6$, whereby D_L represents the diameter of the heart at long-axis image and D refers to the diameter of the heart at short-axis images. ESV was calculated with the same

principle except that the diameters were measured at systole. Stroke volume (SV) was calculated as SV= EDV-ESV and cardiac output (CO) was determined by multiplying SV with the heart rate (HR). Percentage LV ejection fraction (%EF) was calculated as %EF= (EDV-ESV)/EDV × 100 (%). Percentage LV fractional shortening (%FS) was calculated as %FS= (Dd-Ds)/Dd × 100 (%). Dd represents the diameter of the heart at diastole at short-axis images and Ds refer to the diameter of the heart at systole. Images were analyzed with EchoPac Software.

2.3.4 Isolation of the heart and kidney

At sacrifice, heart and kidney were explanted for further analysis. Briefly, the rats were anesthetized with Nembutal (50 mg/kg i.p) and heparin (2000 u/kg) was injected i.p to prevent coagulation of blood. The heart was quickly excised and placed in cold Tyrode solution immediately with the following composition (in mM): 137 NaCl, 5.4 KCl, 0.5 M MgCl2.6Aq, 1 CaCl2, 11.8 (Na)HEPES, 10 glucose and 20 taurine adjusted to pH = 7.4 with HCl. The LV was weighted after heart perfusion with Tyrode solution and excised into small pieces. Next, the ventricle was incubated in liquid nitrogen and grinded into powder.

The kidneys were isolated quickly and the weight was determined. Next, the membrane of one kidney was removed. Half of the kidney (obtained through a mid-section) was snap-frozen in liquid nitrogen and grinded into powder for subsequent protein extractions. All samples were frozen at -80°C.

The remaining heart and the other half of the kidney was immersed in 4% PFA solution, followed by incubation in 70% ethanol. These samples were further processed into paraffin coupes for immunohistochemical evaluation.

2.3.5 Detection of AGE, RAGE and sRAGE expression in LV and kidney by western blot assay

Protein extracts for analyses of AGE and RAGE were prepared from frozen hearts and kidneys powdered in liquid nitrogen-cold mortar. Equal amounts of powder from different animals were resuspended in RIPA buffer (50 mM Tris pH 7.4, 150 mM NaCl, 1 mM EDTA, 1% NP-40, 0.25% Sodium-deoxycholate and 1 tablet protease inhibitor ROCHE). The substances Tris, NaCl and EDTA were purchased from AnalaR Normapur® (Belgium). Sodium-deoxycholate and NP-40 were obtained from Sigma-Aldrich® (Belgium). The protein

concentration of each sample was determined by means of standard curves generated using the BSA standards (0, 25, 125, 250, 500, 750, 1000, 1500 and 2000 µg/mL) and Pierce™ BCA Protein Assay Kit (Thermo Scientific, Belgium). For immunoblot analysis, equal amounts (20 µg/lane or 10 µg/lane) of proteins were electrophoresed on SDS-PAGE. Acrylamide and bis-acrylamide were purchased from Merck Millipore (Belgium). Each sample was diluted with reducing buffer consisting of MilliQ, 0.5 M Tris-HCl (pH 6.8), glycerol, 10% SDS and 1% bromophenol blue. The samples were heated 4 min at 95°C. To ensure equal sample loading, the ratio of band intensity to β-actin was obtained to quantify the relative protein expression level. BIORAD Precision Plus Protein Standards Dual Color (BIO-RAD, Belgium) was used to visualize the molecular weight of the proteins of interest. The gels were run at 200 V in SDS running buffer consisting of 25 mM Tris, 0.192 M glycine and 0.1% SDS (pH 8.3). Next the proteins were transferred on a PVDF membrane (Merck Millipore, Belgium) in transfer buffer at 350 mA for 90 min. After transferring, membranes were blocked during 2h in 5% BSA, 10% serum in TBS-T. The membranes were incubated overnight with the primary antibody at 4°C. For AGE, an antibody dilution of 1:500 in 2% BSA TBS-T (anti-AGE, Sopachem, Belgium) and for RAGE, an antibody dilution of 1:1000 in 2% BSA TBS-T (anti-RAGE, Santa Cruz Biotechnology®, Germany) was used. β-actin was incubated with a antibody dilution of 1:2500 in 2% BSA TBS-T (Santa Cruz Biotechnology®, Germany). Next, the membrane was incubated 2h with the secondary antibody at room temperature. A rabbit anti-mouse HRP conjugated secondary antibody dilution of 1:2500 in 2% BSA TBS-T was used for β-actin (Dako, Belgium). Polyclonal rabbit anti-mouse HRP (Dako, Belgium) secondary antibody dilution of 1:2000 in 2% BSA TBS-T was used for AGE. For RAGE, polyclonal goat anti-rabbit HRP (Dako, Belgium) secondary antibody dilution of 1:2000 in 2% BSA TBS-T was used. The immunoreactive bands were identified with the ECL detection kit (Thermo Scientific, Belgium) and visualized with ImageQuant™ LAS 4000 mini. The bands were quantified with the related ImageQuant software (GE Healthcare Life Sciences).

2.3.6 Detection of RAGE expression in LV by immunohistochemistry

The isolated hearts underwent a postfixation in 4% PFA in PBS (1h, 4°C) followed by a incubation in 70% ethanol (overnight, 4°C). In brief the LV was processed and embedded in paraffin followed by sectioning (8 µm in thickness). The sections underwent deparaffinization. The slides were washed 3x5 minutes with PBS followed by incubation with

0.3% PBS/H_2O_2 (Sigma-Aldrich®, Belgium) for 10 min to block the endogenous peroxidase. After a second wash with PBS, the slides were blocked during 60 min with 20% protein block (Dako, Belgium) in PBS-T at room temperature for blocking non-specific binding. Next, the slides were incubated overnight at 4°C with the primary rabbit anti-rat antibody for RAGE (Santa Cruz Biotechnology®, Germany) diluted 1:250 in PBS-T protein block. Following washing in PBS, sections were treated for 60 min at room temperature with the secondary antibody biotinylated swine anti-rabbit (Dako, Belgium) diluted 1:400 in PBS-T protein block. Next, the slides were washed in PBS 3x5 minutes followed by incubation with a 1:800 streptavidine-HRP (Dako, Belgium) dilution in PBS for 30 min. The peroxidase activity was visualized by treating the slides with DAB (Dako, Belgium) for 10 min followed by 30 sec hematoxyline counterstaining. Following dehydration, mounting was performed with the mounting medium DPX (Merck Millipore, Belgium). Visualization was performed with the MIRAX scanner (Zeiss Microsystems, Germany). Scanned LV and kidney sections were analyzed using a semi-automated procedure programmed for the AxioVision software package. Identical settings were used for all images.

2.3.7 Detection of fibrosis in LV and kidney by Picrosirius Red staining

LV and kidney tissue were processed and embedded in paraffin followed by sectioning (8 µm and 9 µm in thickness, respectively). The sections underwent deparaffinization followed by incubation for 1h with Picrosirius Red (Fast Green, Chondrex, UK) in order to stain collagen. After extensive washing with distilled water, mounting was performed with the mounting medium DPX (Merck Millipore, Belgium). The visualization was performed with the MIRAX scan as mentioned in the previous section. From all LV stainings, 4 regions were selected in order to quantify collagen content. The same protocol was used to quantify cortical and medullar collagen.

2.3.8 Urine analysis

Baseline urine and urine after 6 weeks of treatment was collected and stored as mentioned before. These samples were analyzed for several parameters by specialized members of the laboratory Ziekenhuis-Oost-Limburg (ZOL) Genk. These parameters levels included glucose, total protein, creatinine, albumin/creatinin, sodium, potassium, chlorides, urea, uric acid and osmolality.

2.4 STATISTICAL ANALYSIS

Data are represented as mean ± standard deviation (SD). Statistical analysis was performed using GraphPad Prism5 software. Means among relative fluorescence intensities of the control and AGEs samples were compared using Kruskal-Wallis one-way ANOVA test followed by Dunn's Multiple Comparison test. Means among baseline values and values after treatment in echocardiography measurements and CML measurements were compared using Student paired *t*-test. Means among males and females in echocardiography and CML measurements were compared using the Student unpaired *t*-test. $P < 0.05$ was considered as significant.

3 RESULTS

3.1 Incubation of BSA with glycolaldehyde *in vitro* generates AGEs

Since there are several ways to prepare AGEs *in vitro*, we prepared the AGEs at our research department. The AGEs formed rapidly within 5 days of incubation of 7 mg/mL BSA with 90 mM glycolaldehyde at 37.1°C. The formation of AGEs was validated by means of coomassie staining and fluorescence measurements. The fluorescence intensity of the home-made AGEs was compared to a purchased positive control, made on glycolaldehyde-basis. The AGE-BSA exhibited a characteristic emission at 460 nm on excitation at 370 nm (51). The fluorescence spectra of AGE-BSA showed fluorescence intensities higher than those of the respective control BSA sample (incubated without glycolaldehyde at 37.1°C), indicating protein glycation and cross-linking. The fluorescence values of AGE-BSA and the positive control revealed comparable relative fluorescence intensity as shown in Fig. 5A. The relative fluorescence intensity in AGE-BSA samples was significantly higher compared to the control ($P<0.05$). There was no significant difference in relative fluorescence intensity between the AGE-BSA solutions and the positive control. BSA, which serves as the control solution, contained monomers as well as dimmers as demonstrated in Fig. 5B. Coomassie staining showed also that the AGE-BSA samples contained high-molecular weight proteins identical at the top of the gel, which is also observed in the positive control. In addition, positive control contained also BSA monomers that were not cross-linked. This event was absent in the AGE-BSA sample meaning stronger cross-link formation.

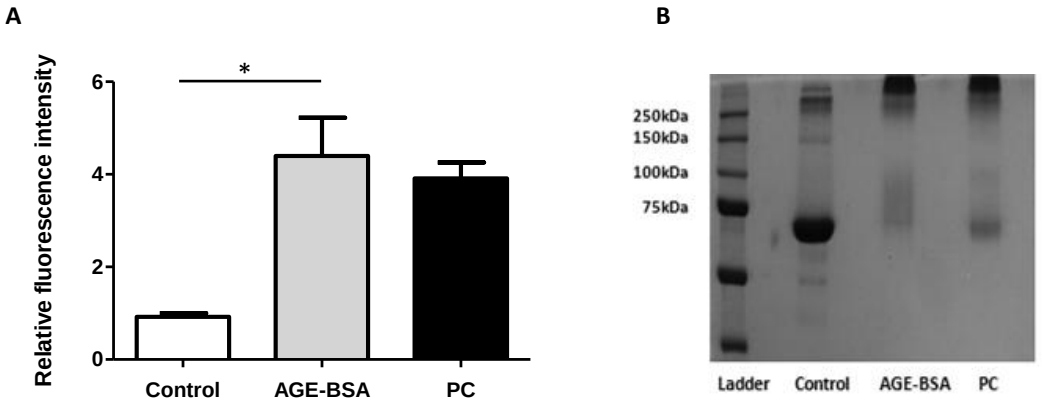

Figure 5: Validation of AGE-BSA formation *in vitro*. (**A**) Increased relative fluorescence intensity of BSA-modified AGEs to the same extent as commercially available AGEs. The fluorescence intensity of the home-made AGE-BSA (n=5) is approximately 4 times higher in comparison to the control sample (BSA; n=5) (**B**) Same pattern of BSA-modified AGEs compared to the PC. PC: positive control *P<0.05 vs control

3.2 Body weight is not changed after AGE-BSA injections

All animals gained weight normally during the entire study period. One AGE-BSA injected male rat died after 5 weeks, limiting the sample size to n=4. The body weight (BW) at baseline was not different for males and females. However, male controls as well as AGE-BSA treated male rats gained clearly more weight in comparison to their female counterparts as shown in Fig. 6. Specifically, the mean BW differed between males and females after 2, 4 and 6 weeks of treatment, indicating males gaining faster weight than females. AGE-BSA treatment for 6 weeks did not affect the mean BW since the animals in the control group and AGE-BSA treated group gained weight equally during the entire experiment. However, a slight decrease in BW was present in male rats injected with AGE-BSA at the end of the experiment (497±42 g) compared to the male control group (557±37 g) as shown in Fig. 6.

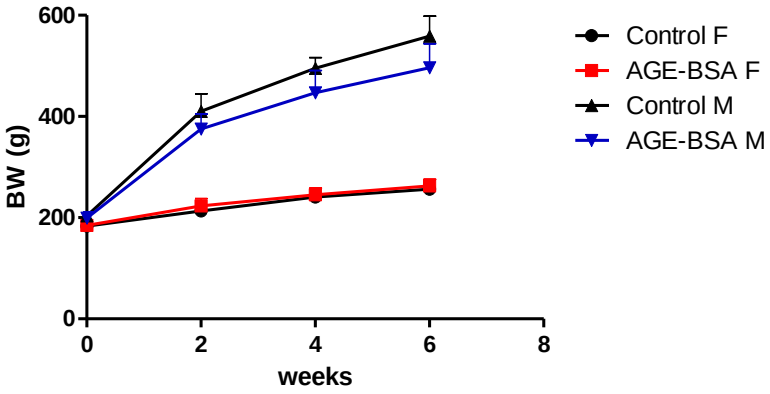

Figure 6: Effect of AGEs injections on the BW evolution of male and female rats. It should be noted that the initial BW for all animals were obtained 3 days before starting the AGE-BSA and control injections. Males (M) gained more weight compared to their female (F) counterparts. AGEs injections had no significant effect on BW in both sexes. Control F: n=2; AGE-BSA F: n=5; Control M: n=2; AGE-BSA M: n=4. BW: body weight.

3.3 AGEs induces cardiac hypertrophy in male and female rats

Daily injections of AGE-BSA over a period for 6 weeks resulted in cardiac dysfunction in both genders. Basic morphological and functional parameters were measured to assess cardiac function as shown in table 1. In addition, male rats showed dilatation of the hearts on echocardiography indicating that cardiac dysfunction in males injected with AGE-BSA was more pronounced compared to the AGE-BSA treated females.

Table 1: Echocardiography parameters after 6 weeks AGE-BSA injections.

Parameter	Baseline F	6wk F	Baseline M	6wk M
AWTd (mm)	1.21±0.05	1.73±0.16*	1.34±0.09	1.95±0.07*
PWTd (mm)	1.50±0.13	2.01±0.12*	1.58±0.11	1.99±0.21*
EDV (µl)	138±26	180±12*	157±20	366±54*
ESV (µl)	33±10	44±9	46±13	139±35*
SV (µl)	104±18	136±10*	111±21	227±42*
CO (min/min)	42±6	53±3*	44±9	88±18*
FS (%)	44±5	44±5	38±8	33±4
EF (%)	76±3	75±4	70±8	62±7

AWTd: anterior wall thickness at the end of diastole; PWTd: posterior wall thickness at the end of diastole; EDV: end diastolic volume; ESV: end systolic volume; SV: stroke volume; CO: cardiac output; FS: fractional shortening; EF: ejection fraction; F: female; M: male. *P<0.05 vs baseline

AWTd and PWTd increased significantly in both genders after 6 weeks of AGE-BSA injections compared to baseline values. In addition, the % increase of each parameter after 6 weeks was calculated starting from the baseline values. The % increase in AWTd (46%) of AGE-BSA treated males was higher compared to AGE-BSA treated females (43%), indicating more hypertrophy in males. Relaxation and contractility properties of the heart were assessed by measurement of EDV and ESV, respectively. The mean EDV in both genders injected with AGE-BSA increased significantly after 6 weeks. The % increase in EDV after 6 weeks compared to baselines in males (133%) was higher than for females (30%). The mean ESV was only significantly different in males upon AGE-BSA treatment. These results suggest that an increased force has to be generated in order to pump blood through the whole body. SV and CO were significantly elevated in both genders compared to their baseline values. Again, the % increase of SV in males (105%) and CO (100%) was higher than females SV (31%) and

CO (26%). Global function was assessed by measurement of EF and FS. These parameters did not changed significantly after 6 weeks of treatment in both genders. These findings suggest diastolic heart failure due to AGE-BSA injections since the animals show preserved EF.

3.4 Hypertrophy is more pronounced in males

A series of parameters were measured after sacrificing the animals at the end of 6 week injections. These parameters included the BW, heart weight (HW), LV weight (LVW), tibia length (TL), and lungs weight (LW) as demonstrated in table 2. Males were approximately twice the size of female rats as mentioned before. LW was estimated in order to evaluate congestion profile after AGE treatment since presence of CHF may cause pulmonary edema. This event also occurs in heart failure animal models subsequent to myocardial infarction.

Table 2: Measured parameters of the experimental groups at sacrifice.

Parameter	Control F (n=2)	AGE-BSA F (n=5)	Control M (n=2)	AGE-BSA M (n=4)
Sacrifice BW (g)	256±18	263±16	557±37	497±42
HW (mg)	940±7	840±40	1415±7	1535±161
LVW (mg)	650±14	608±17	1130±141	1070±118
TL (cm)	3.65±0.07	3.68±0.26	4.7±0.7	4.08±0.3
LW (g)	1.44±0.02	1.29±0.16	2.26±0.08	1.89±0.14

BW: body weight; HW: heart weight; LVW: left ventricle weight; TL: tibia length; LW: lungs weight; F: female; M: male.

LW was normalized to BW and TL. At 6 weeks after AGE-BSA treatment, there was a substantially decrease in LW after AGE-BSA treatment in both genders as shown in Fig. 7A and 7B, indicating that AGE-BSA injections caused no pulmonary congestion. Since measuring the HW of the animals is not representing the correct estimation for cardiac hypertrophy, HW was corrected for the BW of the animal as shown in Fig. 7C. The HW-to BW ratio was higher in control females (n=2) compared to AGE-BSA injected females (n=5). AGE-BSA treated males (n=4) showed substantially increased hypertrophy compared to the control males (n=2). Moreover, the ratios HW-to TL was measured for profiling myocardial hypertrophy as demonstrated in Fig. 7D. Interestingly, AGE-BSA treated males showed substantially increased hypertrophy compared to their AGE-BSA injected female counterparts by normalizing to TL.

Because statistical analysis is not possible in this setting no clear statement can be made whether the observed differences are statistically significant.

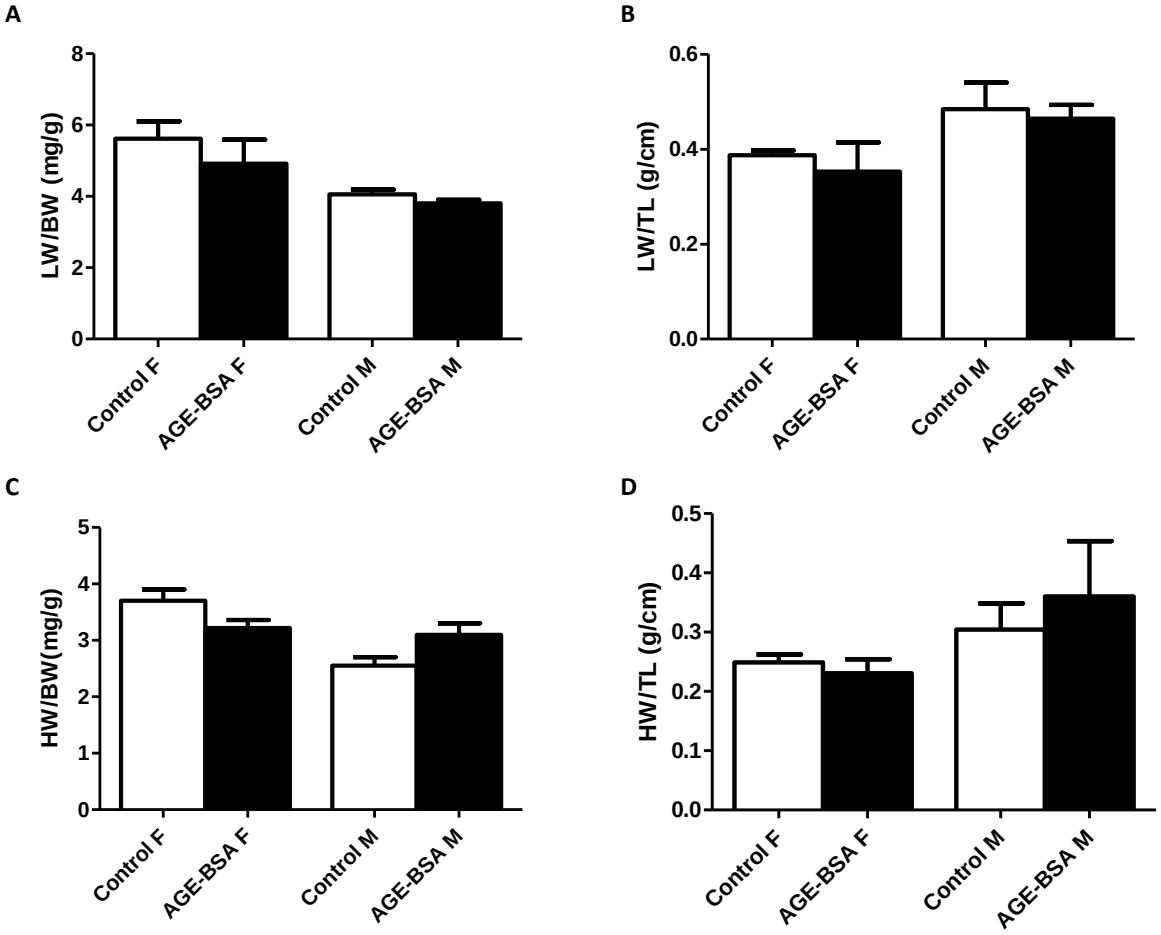

Figure 7: Pulmonary congestion and cardiac hypertrophy profiling. (**A**) Lung-to-body weight ratio (mg/g) and (**B**) lung-to-tibia length ratio (g/cm) decreased slightly in AGE-BSA treated females (n=5) compared to the control group (n=2) and in AGE-BSA treated males (n=4) compared to control (n=2). (**C**) Heart-to-body weight ratio (mg/g) in females decreased slightly in the AGE-BSA treated group compared to the control group and increased in AGE-BSA injected males, indicating more pronounced hypertrophy in males compared to the control males. (**D**) heart-to-tibia length ratio (g/cm) in AGE-BSA treated males is substantially increased compared to the AGE-BSA treated females. LW: lungs weight; HW: heart weight; TL: tibia length; F: female; M: male.

3.5 AGE-BSA injections cause an increased collagen in LV and kidney

Since AGEs can alter the myocardial and renal structure, collagen content was evaluated in both organs after AGE-BSA injections for 6 weeks. Total collagen was measured in LV and kidneys from control and AGE-BSA injected animals as demonstrated in the representative Fig. 8A and Fig. 9. Based on Picrosirius red staining, pixels were calculated for total collagen staining, as indicated by red coloring, and normal tissue, colored green. Total collagen in LV was increased in both genders treated with AGE-BSA compared to the control groups

indicating fibrosis. In general, males showed higher collagen contents than females since collagen is related to the HW as shown in Fig. 8B. AGE-BSA injected males showed substantially increase in total collagen when compared to the AGE-BSA injected females. Representative images for LV collagen staining are demonstrated in Fig. 8C.

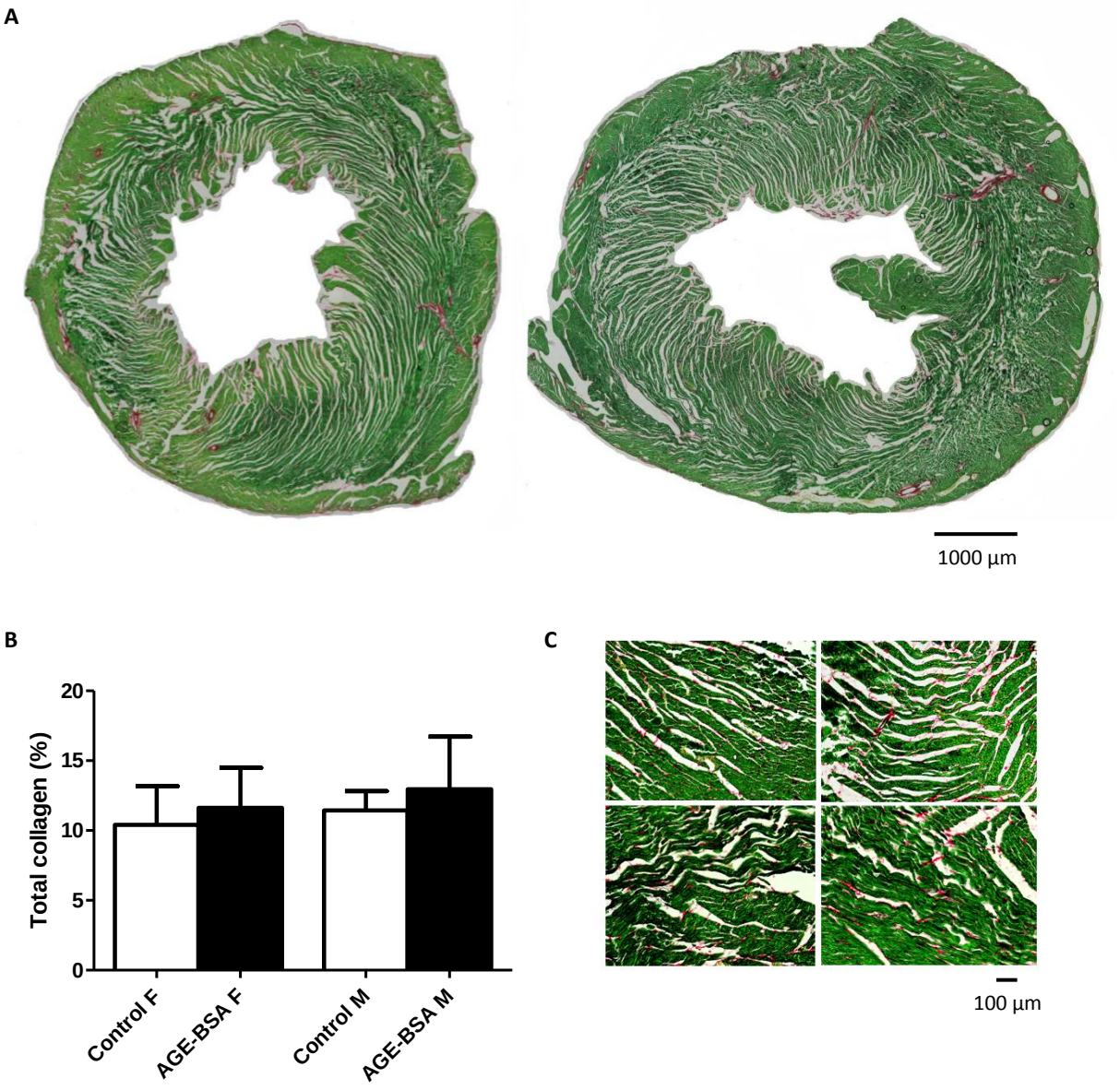

Figure 8: AGE-BSA injections cause an increased collagen in LV. (**A**) Representative midaxillary LV images of females (left image) and males (right image). (**B**) Total collagen (%) in LV stained with Picrosirius Red increased substantially in both genders after AGE-BSA treatment. The ratio of total collagen to the LV area was calculated from 4 randomly selected fields in individual sections. (**C**) Representative Picrosirius Red stainings (20x) of LV from control female (upper left), AGE-BSA female (upper right), control male (bottom left) and AGE-BSA male (bottom right). F: female; M: male.

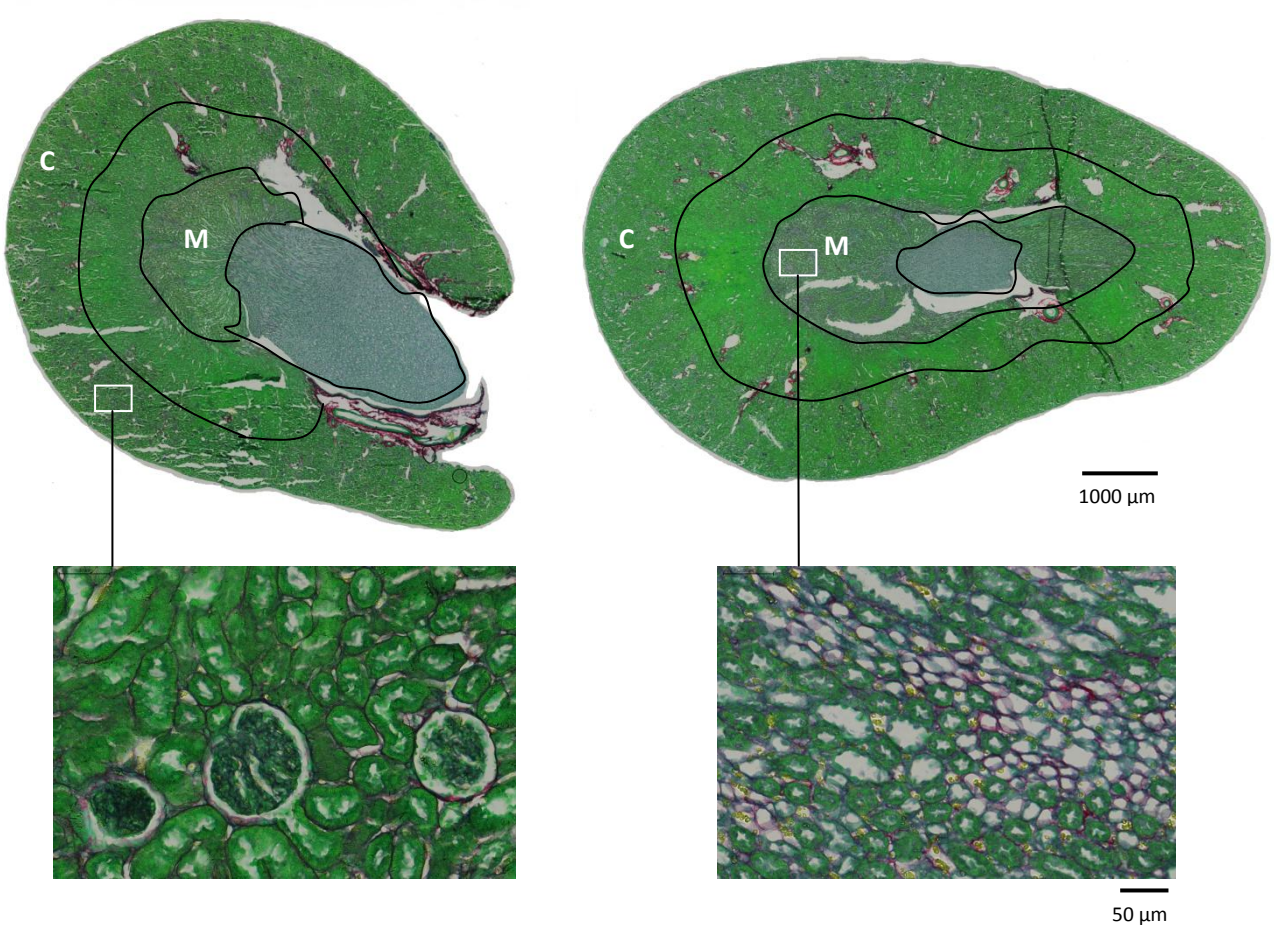

Figure 9: Kidney morphology as indicated by Picrosirius Red staining. Representative images of the kidney from female rats (left image) and male rats (right image). Collagen content was measured in the cortex region (C) and in the medullar region (M). A correct orientation was obtained for the cortex by selecting regions including glomeruli. Magnification: 40x.

Identical findings were found for the kidney collagen. Cortical and medullar interstitial collagen was measured separately since these regions show differences in the residing structures with different functions. Fig. 9 shows representative kidney images and the selected cortical and medullar regions. Collagen was higher concentrated in the medulla compared to the cortex of control animals. The interstitial collagen (%) in the cortex of AGE-BSA injected females (12.9%) was higher compared to the controls (5.3%) as demonstrated in Fig. 10A. AGE-BSA treated males had higher collagen in the cortex (11.8%) compared to the control males (4.2%). The interstitial collagen (%) in the medulla was increased in AGE-BSA treated females (21.6%) compared to control females (14.23%) as demonstrated in Fig. 10B. Also here, AGE-BSA treated males showed higher collagen in the medulla (21.5%) compared to the controls (16%).

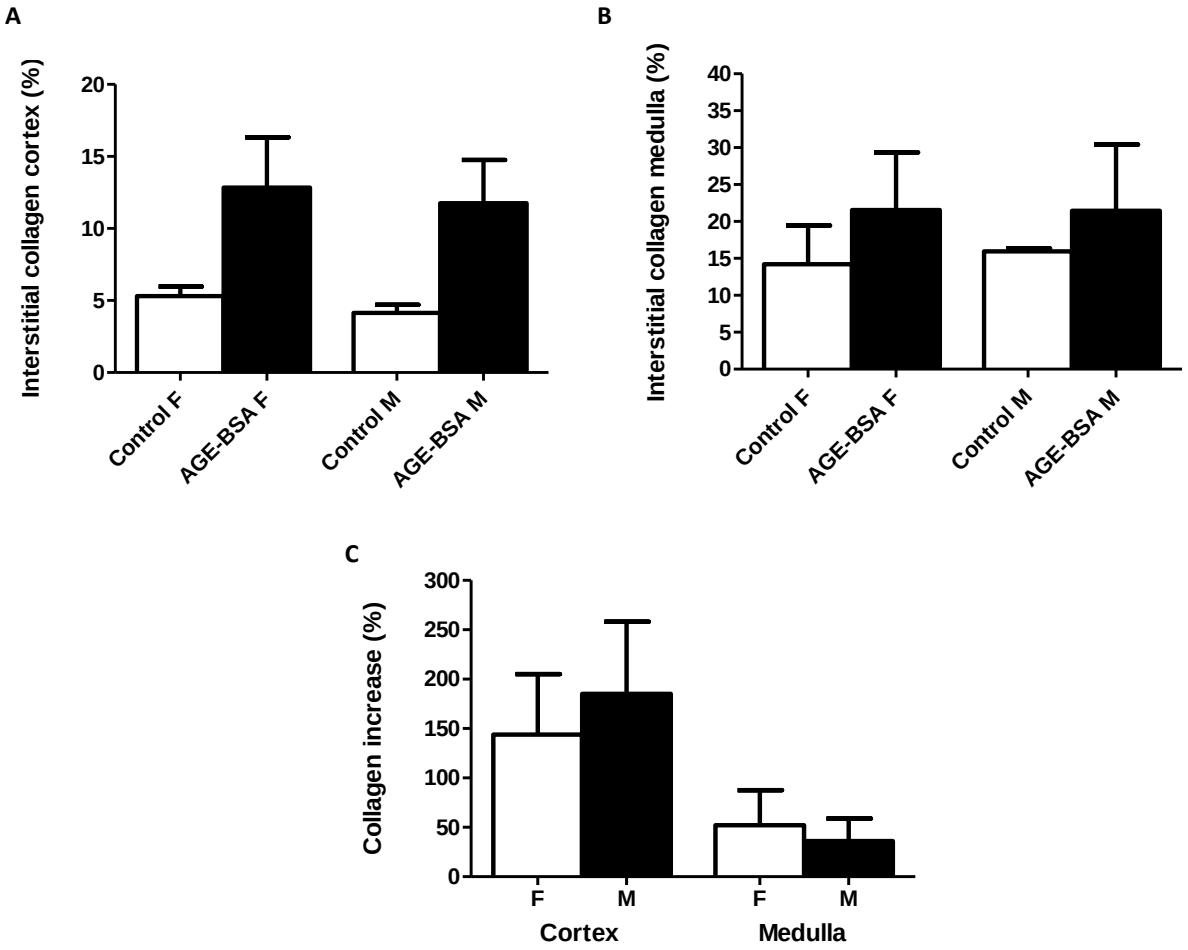

Figure 10: Fibrosis is more pronounced in the cortical region of the kidney in AGE-BSA injected animals. (**A**) Collagen is increased in the interstitial cortical region in AGE-BSA injected animals compared to the controls. (**B**) Collagen is substantially increased in the interstitial medulla in AGE-BSA injected animals. (**C**) The percentage of collagen increase is more pronounced in the cortex in both genders. F: female; M: male.

In order to investigate which region in the kidney is more affected by AGE-BSA injections, the percent increases were calculated in both regions for both genders. In the cortical region, females showed collagen increases of 142% and males up to 184% after 6 weeks AGE-BSA injections. The collagen increases in the medullar region for females was 52% and for males 37%. Fig. 10C show that the collagen increase (%) in the cortex is higher than the collagen increase in the medulla for both genders indicating that the cortical region developed more pronounced fibrosis compared to the medullar region due to AGE-BSA injections.

3.6 Circulating AGE-protein CML is increased in males after 6 weeks of AGEs injections

One of the specific AGEs molecules CML was measured in serum samples obtained at baseline and after 6 weeks of treatment as shown in Fig. 11A. The serum levels (ng/mL) of CML in male Sprague-Dawley rats at baseline and after 6 weeks of AGEs injections were 698±453 (n=6) and 1878±1887 (n=4), respectively. There was no statistically significant difference between the baseline and AGEs treated males. However, a clear increasing trend after AGEs injections in males is present. Females did not show significant differences between the different time points. The serum levels (ng/mL) of CML in female Sprague-Dawley rats at baseline and after 6 weeks of AGEs injections were 3874±2437 (n=6) and 3407±1564 (n=5), respectively. It was remarkable that here was a clear difference between mean baseline values of CML in males (698±453 ng/mL) and in females (3874±2437 ng/mL).

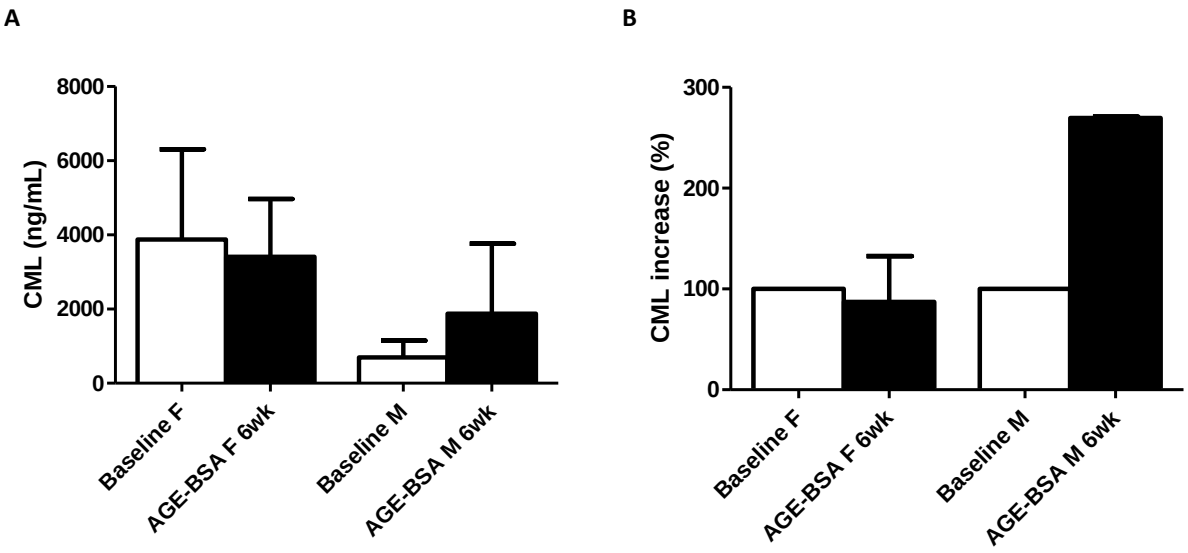

Figure 11: CML concentration in rat serum among the different groups. (**A**) Mean CML concentration (ng/mL) in serum obtained at baseline (n=7) and after 6 weeks of AGEs injections (n=5) for females and for males baseline (n=6) and AGEs injections (n=4). There is an increasing trend in CML concentration in males with the evolution of time. The CML concentration is not different in AGE-BSA injected females after 6 weeks compared to baseline. Data are represented as mean ± SD. (**B**) % increase of CML is pronounced in AGE-BSA treated males while there are no differences in AGE-BSA injected females after 6 weeks. F: female; M: male.

In addition, % increases of CML were calculated compared to baseline values. After 6 weeks, CML in AGE-BSA females decreased with 12% compared to baseline values indicating that a longer period of injection would result in increased CML. However, the CML increase in AGE-BSA injected males was already pronounced (269%) after 6 weeks injections.

3.7 AGE expression in rat cardiac tissue is increased in AGE-BSA treated females

Increased levels of AGEs upregulate own expression, an example of positive-feedback activation. This event occurs when RAGE expression is increased due to increased AGEs levels. Upregulation of RAGE in his turn increases ROS amount, which causes even more generation of AGEs. Analysis was performed in order to evaluate AGEs expression in LV after AGE-BSA injections for 6 weeks. Western blot analysis was performed in order to quantify the protein levels of AGE in cardiac tissue, more specific in the LV. All expression levels are corrected to the reference protein β-actin. The analyzed levels are demonstrated in Fig. 12A, with the corresponding representative results from the western blot shown in Fig. 12B. AGE expression is increased in females treated with AGE-BSA (n=5) compared to the control group (n=2). In contrast, AGE-BSA injected males (n=4) show lower AGE expression compared to the control injected males (n=2). Interestingly, AGE expression in males and females after 6 weeks AGE-BSA injections were of the same level. The performed western blots for AGE expression show bands at approximately 75kDa and for β-actin at approximately 43kDa as shown in Fig. 12B.

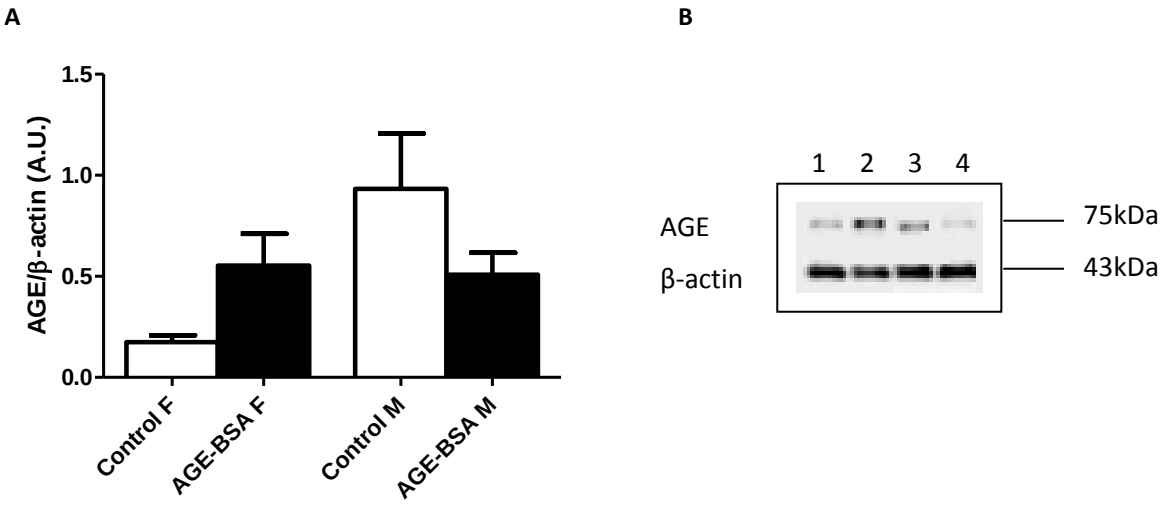

Figure 12: AGE expression is increased in AGE-BSA injected females. (**A**) Western blot analysis show that the AGE expression tend to increase after AGE-BSA injections in females. AGE expression is decreased in AGE-BSA injected males. (**B**) Representative results from the western blotting. AGE was detected at 75kDa and β-actin at 43kDa. Lane 1: Control F; Lane 2: AGE-BSA F; Lane 3: Control M and Lane 4: AGE-BSA M; F: female; M: male; A.U.: arbitrary units.

3.8 RAGE and sRAGE expression in LV is increased in AGE-BSA injected females

RAGE expression was evaluated with immunohistochemical staining. Visually, evaluation of selected LV sections showed more intense RAGE staining in both genders treated with AGE-BSA compared to the control groups as shown in Fig. 13A but data are not quantified. Next, western blotting showed increased RAGE and sRAGE expression in AGE-BSA treated females as demonstrated in Fig. 13C and 13D. There was no increase in RAGE or sRAGE expression in AGE-BSA treated males, contradicting the RAGE staining. Representative bands detected at 55kDa (full length RAGE) and 41kDa (sRAGE) are demonstrated in Fig. 13B.

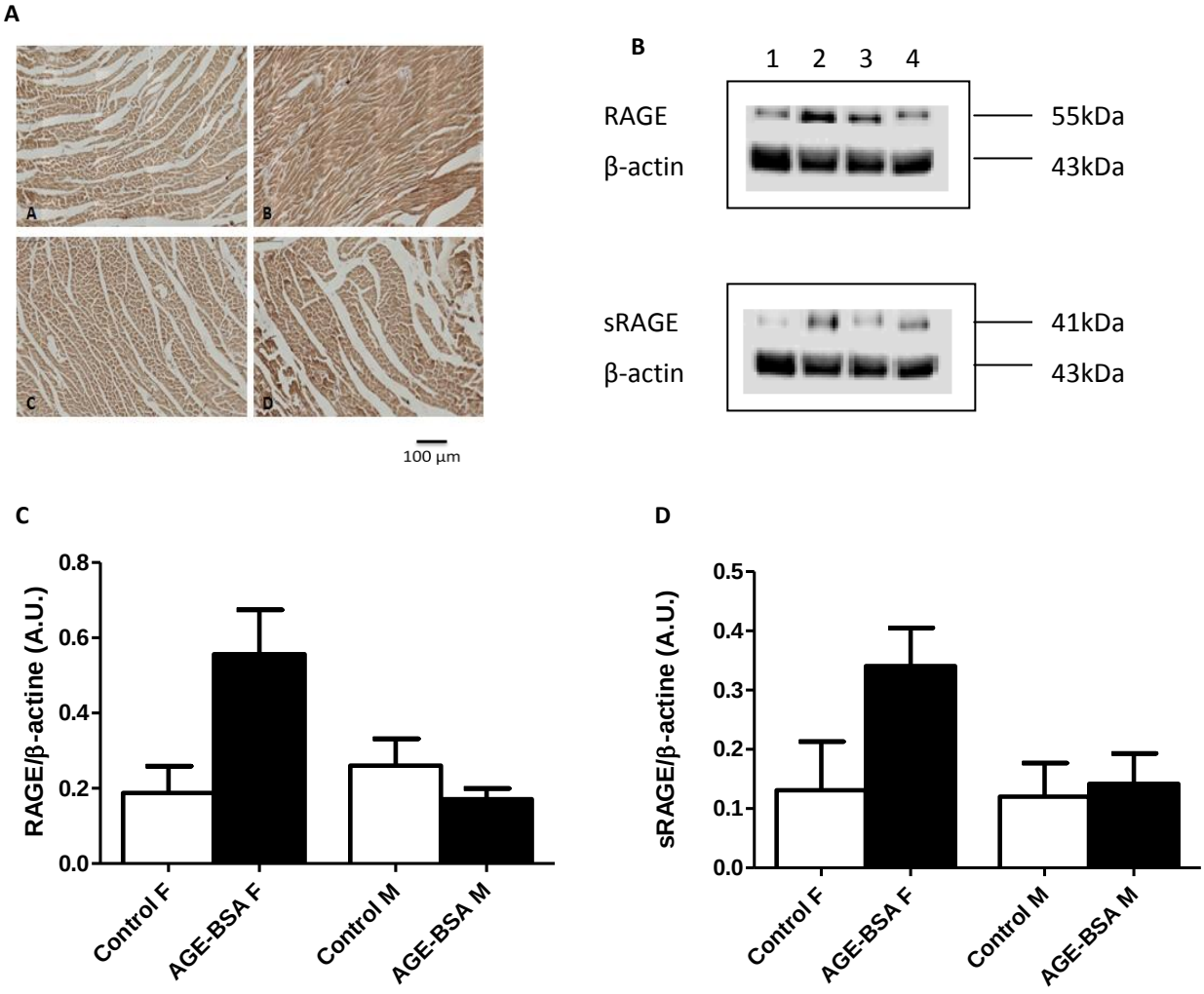

Figure 13: RAGE and sRAGE expression in LV is more pronounced in AGE-BSA treated females as shown by western blotting. (**A**) Representative DAB staining images (20x) of LV from (A) control female (n=2), (B) AGE-BSA female, (n=5), (C) control male (n=2) and (D) AGE-BSA male (n=4). (**B**) and (**C**) Western blot analysis show that RAGE and sRAGE expression increased in females after AGE-BSA injections. Bands were detected at approximately 55kDa and 41kDa, respectively. Lane 1: Control F; Lane 2: AGE-BSA F; Lane 3: Control M and Lane 4: AGE-BSA M; F: female; M: male; A.U.: arbitrary units.

3.9 KIM-1 decreased in AGE-BSA injected animals at 6 weeks

In order to evaluate kidney damage, a urinary biomarker KIM-1 was measured in urine, which is an early indicator of tubular injury. KIM-1 is decreased in AGE-BSA injected females (53.64 ng/mg_{crea}) and males (48.13 ng/mg_{crea}) as shown in Fig. 14. Baseline KIM-1 level was higher in females (146.3 ng/mg_{crea}) compared to mean KIM-1 baseline value for males (82.94 ng/mg_{crea}). Furthermore, KIM-1 levels in AGE-BSA treated males and females were of the same level at 6 weeks treatment.

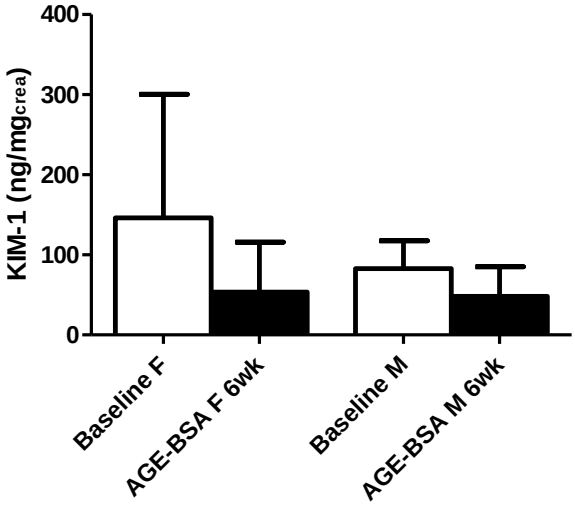

Figure 14: KIM-1 is decreased after 6 weeks AGE-BSA injections in both genders. Mean KIM-1 concentration in urine obtained at baseline (n=6) and after 6 weeks of AGEs injections (n=5) for females and for males baseline (n=6) and AGEs injections (n=4). There is a decrease in KIM-1 urine concentration in both genders with the evolution of time. The KIM-1 concentration is not different in AGE-BSA injected animals after 6 weeks treatment. Data are represented as mean ± SD. Values are corrected per mg creatinine (mg_{crea}). F: female; M: male; wk: weeks.

3.10 RAGE expression in AGE-BSA injected males is increased in the kidney

RAGE expression was measured in kidney protein extracts since this receptor is involved in the development of fibrosis in the interstitial region upon increased AGEs. AGE-BSA injected males showed higher RAGE expression compared to the control group as demonstrated in Fig. 15A. Remarkably, RAGE expression was not increased in AGE-BSA injected females after 6 weeks. In kidney, only full length RAGE was detected at 55kDa as shown in Fig. 15B.

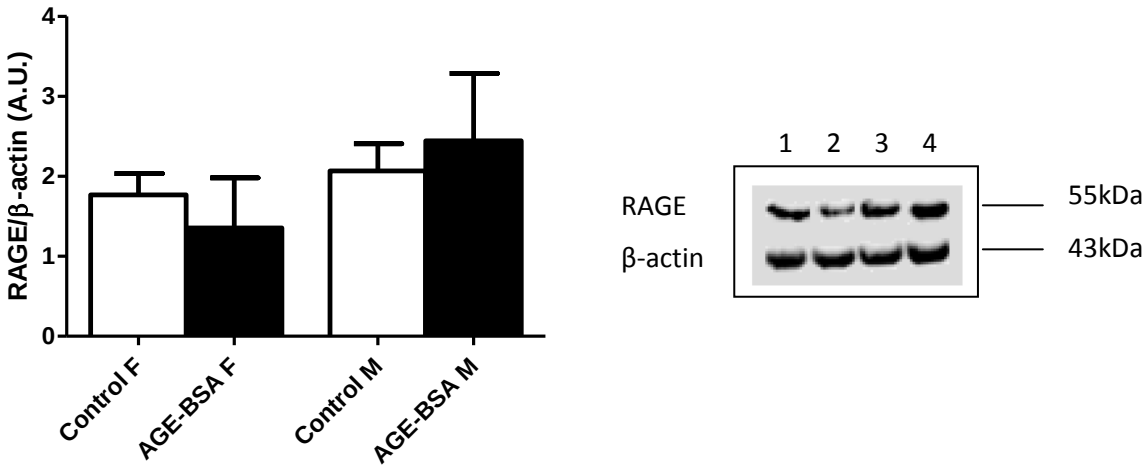

Figure 15: RAGE expression in kidney is increased in AGE-BSA injected males. (**A**) Western blot analysis show that RAGE expression increased in AGE-BSA treated males. (**B**) Representative bands for RAGE detected at approximately 55kDa and β-actin at 43kDa. Lane 1: Control F; Lane 2: AGE-BSA F; Lane 3: Control M and Lane 4: AGE-BSA M; F: female; M: male; A.U.: arbitrary units.

3.11 AGE-BSA injected animals showed normal glucose levels after 6 weeks AGEs injections

Urine analysis was performed by specialized members of the laboratory ZOL in order to investigate kidney functioning related to AGE-BSA injections. The parameters that were measured in urine are listed in table 3. Since prolonged injections of AGEs can disturb the glycaemic status, glucose levels would provide information whether the animals reached hyperglycaemia or not since AGEs are injected modified sugars. Results showed that glucose levels in urine remained unchanged upon 6 weeks AGE-BSA injections in both genders. Furthermore, basic parameters were measured related to the kidney functioning. There was no change in creatinine concentration in urine after 6 weeks AGE-BSA injections in both genders. However, a substantially increase in creatinine was present in control females after 6 weeks of BSA injections. AGE-BSA or control injections did not affect microalbumin, albumin, total protein levels and osmolality in urine. These results show that the filtering and

concentrating capacity of the kidney is not deregulated after 6 weeks of treatment. Moreover, since the kidneys maintain the proper balance of water and minerals, electrolyte concentrations were measured. Sodium, potassium and chlorides tended to decrease in AGE-BSA injected males, while no changes were observed in females. Changes in ion levels indicate that the reabsorbing capacity of the kidney may be influenced by AGEs. Furthermore, one of the main waste products, urea, was measured since it provides information about the filtration and excretion capacity of the kidney. Urea levels were slightly increased in all animal groups. Finally, uric acid concentration was determined in urine. Uric acid levels tended to decrease in all animal groups after 6 weeks indicating over compensatory working activity of the kidneys.

Table 3: Parameters analysed in urine.

Parameter	Control F bl (n=2)	Control F 6wk (n=2)	AGE-BSA F bl (n=4)	AGE-BSA F 6wk (n=4)	Control M bl (n=2)	Control M 6wk (n=2)	AGE-BSA M bl (n=3)	AGE-BSA M 6wk (n=3)
Glucose (mg/mg_{crea})	4.10^{-3}±6.10^{-3}	3.10^{-3}±4.10^{-3}	8.10^{-3}±3.10^{-3}	3.10^{-3}±3.10^{-3}	5.10^{-3}±7.10^{-3}	5.10^{-3}±8.10^{-3}	9.10^{-3}±4.10^{-3}	9.10^{-3}±4.10^{-3}
Creatinine (mg/dL)	77±55	104±82	88±29	69±11	76±32	73±27	74±3	72±11
Microalbumin (mg/mg_{crea})	3±0	1±1	3±1	2±1	1±1	1±1	2±1	1±0
Albumin (mg/L)	6±4	6±0	18±4	13±17	3±2	1±1	10±10	2±2
Total protein (mg/mg_{crea})	38.10^{-2}±6.10^{-2}	57.10^{-2}±6.10^{-2}	76.10^{-2}±22.10^{-2}	54.10^{-2}±8.10^{-2}	2±0	1±0	1±0	1±0
Albumin/Creatinine (mg/g)	36±0	15±11	34±12	29±9	15±6	11±12	23±6	8±3
Sodium (mEq/mg_{crea})	17±1	16±4	17±1	17±2	21±2	11±1	24±3	11±0
Potassium (mEq/mg_{crea})	30±9	25±8	26±2	26±1	36±7	23±4	37±1	23±1
Chlorides (mEq/mg_{crea})	25±4	23±3	23±3	24±2	31±1	18±0	39±8	18±0
Urea (mg/mg_{crea})	68±11	77±15	60±3	77±3	51±4	59±12	50±1	60±2
Uric acid (mg/mg_{crea})	14.10^{-2}±9.10^{-2}	1.10^{-1}±1.10^{-1}	18.10^{-2}±3.10^{-2}	17.10^{-2}±2.10^{-2}	25.10^{-2}±13.10^{-2}	17.10^{-2}±6.10^{-2}	22.10^{-2}±4.10^{-2}	16.10^{-2}±4.10^{-2}
Osmolality (mmol/kg H_2O)	1537±841	1438±0	1613±368	1663±242	1638±668	1447±568	1597±69	1372±120

Values are corrected per mg creatinine (mg_{crea}). Data are represented as mean ± SD. F: female; M: male; bl: baseline; wk: weeks.

4 DISCUSSION

In the present study, we showed that daily AGEs injections in rats caused myocardial dysfunction, i.e. cardiac hypertrophy and left ventricular fibrosis in both genders. Based on changes in echocardiography parameters and collagen quantifications, we showed that myocardial dysfunction is more pronounced in males compared to their female counterpart. Besides, cortical kidney regions of AGE-BSA injected males also showed more pronounced fibrosis compared to females.

Likewise, there is no clear vision which AGEs compositions may be involved in cardiac and kidney disorders. Until now, the formation of six distinct AGEs has been established: glucose-derived AGEs, glyceraldehydes-derived AGEs, glycolaldehyde-derived AGEs, methylglyoxal-derived AGEs, glyoxal-derived AGEs and 3-deoxyglucosone-derived AGEs. There are several ways to prepare exogenous AGEs and many articles are published with either different AGEs preparation protocols, indicating that there is no consensus in making AGEs. The presence of large-molecular-weight molecules remaining at the top of the gel indicates that the formation of AGE-BSA is caused by formation of cross-linked proteins. However, our samples did not contain CML or pentosidine since dialyse process eliminated these large-molecular-weight proteins. A solution of AGEs isoforms remained with molecular weights below 300kDa. However, we did not determine the AGEs composition in our samples. In addition, AGEs formation was confirmed with fluorescence measurements, as previously described (52).

In vivo, AGEs are mainly formed during a non-enzymatic reaction between proteins and sugar compounds. However, several other AGEs formation pathways are described. AGEs accumulate in the body with aging and accumulation is accelerated in the presence of diabetes mellitus. In this regard, many researches are focussed on cardiac and renal dysfunction in diabetes. However, there is growing body evidence that AGEs are also related to the development and progression of heart-and kidney failure in non-diabetic patients. Underlying mechanisms remain still unclear. Furthermore, females are more protected against cardiovascular disorders compared to their male counterparts, which has been attributed in part to hormonal differences. Our data are a first step toward understanding the effect of AGEs injections and gender in the modulation of the cardio-renal function.

In this pilot study, cardiac function was assessed by echocardiography measurements. We observed hypertrophy in both genders treated with AGE-BSA as an adaptation to maintain overall function. Moreover, measurements of LV wall thicknesses showed more pronounced hypertrophy in AGE-BSA treated males compared to AGE-BSA treated females. This finding is consistent with previous findings in transaortic constriction animal models, whereby females showed reduced cardiac hypertrophy compared to males (53). This event is often related to estrogens. It has been previously reported that in ovariectomized mice subjected to pressure overload hypertrophy, estrogen replacement attenuated the hypertrophic response (54). This observation strongly suggests that estrogen can modulate hypertrophy. Furthermore, AGE-BSA treatment had significantly increased EDV and ESV in both genders compared to control animals. SV was also significantly increased. These findings are consistent with the previous findings in aging Zucker diabetic rats (55) which demonstrated that Zucker diabetic rats exhibited enhanced contractility. Moreover, increased CO in our AGE-BSA injected rats indicated dilatation of the LV, again as a compensatory mechanism to maintain contractile force of the heart. Lastly, EF and FS parameters were measured to investigate the pump/ functional activity of the heart, i.e. systolic function. These parameters differ in the way that EF is calculated based on volumes and FS is a dimensions-based cardiac function parameter. From a theoretical point of view, the percentage of shortening may be a more suitable measure of LV systolic function. No changes in EF or FS were observed after 6 weeks of treatment. One can assume that animals showed diastolic dysfunction since they show preserved EF. Since diastolic dysfunction is characterized by increased LV end diastolic pressure, blood pressures should be measured in the future since valuable information will be obtained concerning type of dysfunction.

Our results indicate furthermore that males have accelerated myocardial changes compared to females. This finding is consistent with the previous results by Douglas *et al.* (7) which demonstrated that male rats with LV pressure overload showed an early transition to heart failure compared to females. Perhaps, the underlying gender differences in body and heart size influence adaptation to myocardial stress. Or, estrogens may be a transcriptional regulator of genes implicated in hypertrophy. This however remains to be further elucidated.

Cardiac hypertrophy was confirmed further with HW/BW ratios, which was increased in AGE-BSA injected animals. This finding is in accordance with the previous findings by

Herrmann *et al.* (56) which demonstrated increased HW/BW ratios in rats that developed volume overload hypertrophy due to arteriovenous fistula. Moreover, we showed that HW/BW ratios were the same for AGE-BSA injected males and females, indicating equal hypertrophy levels. However, this finding was inconsistent with the echocardiography results that showed more pronounced morphological changes in AGE-BSA injected male rats compared to females. Normalizing the HW with TL showed more pronounced hypertrophy in AGE-BSA injected males compared to their female counterparts. Study of animals of different body size and gender is complex, as heart size can vary. We showed that correcting HW with BW in order to measure hypertrophy is not always reflecting the correct status in the animals.

Collagen is the most abundant structure in the heart. It provides strength and flexibility to the muscle. Myocardial collagen is susceptible to AGEs cross-linking during times of increased collagen deposition, such as in LV hypertrophy. In the present study, increased collagen, i.e. fibrosis, was observed in AGE-BSA injected animals. This finding is consistent with a previous finding by Umadevi *et al.* (57) which reported increased fibrosis in AGEs infused rats. They related this finding to TGF-β, which is a cytokine attributed to ECM remodeling and frequently observed in diabetic cardiomyopathy (58). TGF- β was not measured in our pilot study.

The inflammatory cascade evoked by AGE-RAGE interaction ultimately contributes to the increase in oxidative stress, which is implicated in the progression and pathogenesis of cardiac and renal failure. We showed upregulation of RAGE in AGE-BSA treated females. In this regard, the same study by Umadevi *et al.* (57) showed increased RAGE expression after AGEs treatment due to elevated levels of ROS. They explained this finding furthermore by increased TNF-α expression, which is a contributor to myocardial dysfunction. However, RAGE can also be upregulated by estrogens (59). But neither TNF-α nor estrogens were measured in this pilot study. Since debate is still going on about the role of sRAGE in CVD, we showed that sRAGE was more upregulated in AGE-BSA treated females validating the protective role of sRAGE as been described in several animal models (47, 60). Since expression of RAGE is also dependent on the expression of AGEs, we reported that AGEs expression in the heart was only increased in AGE-BSA injected females. In euglycaemic conditions, such as in the present study, AGEs may form as a result of increased oxidative

stress. Therefore, it is important to determine levels of CML since it is a marker of increased oxidative stress and long-term damage to proteins (61). In a previous research by Lieuw-A-Fa *et al.*, findings suggested that plasma CML levels were involved in the acceleration of cardiovascular complications in patients with renal impairment (62). We showed that serum CML concentrations were increased in AGE-BSA treated males after 6 weeks but CML concentrations were not changed in females. However, the CML concentrations even at baseline were much higher compared to males. The increased occurrence of CML in AGE-BSA injected male serum suggests a role for CML as a biomarker for oxidative damage. We could not observe AGEs accumulation unexpectedly but this can be due to increased sRAGE, which may function as a decoy receptor for AGEs.

Relative little is known about the mechanism of renal handling of AGEs beyond that both the glomerulus and the proximal tubule are involved in AGEs filtration and reabsorption, respectively (63). The present study demonstrates that chronic administration of *in vitro*-prepared AGEs to otherwise healthy rats leads to changes in renal collagen levels, which is an event that is also frequently observed in diabetic nephropathy. Moreover, we showed increased collagen in cortical and medullar regions after AGE-BSA injections. Cortical collagen was distinguished from medullar collagen since there are regional differences in residing structures and their functions. In addition, we showed that cortical collagen increase was more pronounced in AGE-BSA treated males. In a previous research by Peleg *et al.*, they showed kidney collagen accumulation both in the cortex and medulla with aging. Above, higher expression of collagen type I in the cortex of old rats was found compared to the medulla (64). The functional significance of this difference needs to be determined by separate studies.

Furthermore, urine analysis showed changing trends in particular. AGE-BSA injections for 6 weeks caused electrolyte disturbance in males. AGE-BSA injected males showed decreased concentrations of sodium, potassium and chlorides in urine since changes in sodium levels go together with changes in potassium and chlorides concentrations. This decrease in ion levels may be explained by increased Na-K-2Cl symporter reabsorption that goes together with increased sodium-dependent glucose transporter activity. However, glycaemia levels did not change in these animals indicating proper functioning of insulin secretion. A recent research by Coughlan *et al.* reported no changes in plasma glucose levels of AGE-RSA

injected rats for 16 weeks (65), meaning that the concentration and composition of the injected AGEs is of great importance regarding changing glucose levels. The reason why this event is only encountered in males has to be further elucidated. Moreover, we observed increased urea levels, being indicators of either increased protein breakdown in the body or increased protein concentration due to the BSA injections. Furthermore, changes in urea transporter expression should be taken into consideration. Likewise, no obvious renal functional parameters indicating renal damage, e.g., creatinine clearance, proteinuria, albuminuria, were influenced by 6 weeks treatment with either AGE-BSA or control BSA solutions. It should be noted that renal pathology may not be apparent until it is severe. Measurement of urinary glucose may therefore not a good indicator because glucose does not appear in urine until the renal threshold is exceeded. Similarly changes in creatinine clearance, proteinuria and albuminuria probably become apparent only after significant loss of renal function.

Limitations

There were several limitations attached to this study. First, the number of animals in this pilot study was limited. As a result, the study does not had enough statistical power to draw a definite conclusion about gender-differences in cardiac and kidney function outcome due to daily AGEs injections. Besides, the concentration range of injected AGEs and time of injections was not optimized and was based on previous protocols (bron). As a result, early cessation of the injections in this study caused an early stage disease pattern investigation. Second, we could only provide metabolic data at the beginning and the end of the study. Therefore, we have no insight in the urine biomarkers evolution during the AGE injections. Third, comparing the data to previous findings in the literature was limited since this is a pilot study. Therefore, a second non-injected control group will be useful in the future to obtain normal parameters values of proteins such as AGE, RAGE, CML and KIM-1. In the future, blood glucose levels should be measured in order to obtain valuable information about the glycaemia level evolution upon AGEs injections. Besides, it is of great importance in the future setting to apply early and specific biomarkers since early diagnosis of organ dysfunction is needed. A combination of several biomarkers, such as BNP, NT-proBNP, KIM-1 and NGAL, will add value to research since these biomarkers are well associated with early heart-and kidney dysfunction.

5 CONCLUSION AND PERSPECTIVES

In conclusion, the results suggest that AGEs could play a role in the development of fibrosis-induced cardiac and renal dysfunction. Furthermore, findings support that females have a delayed progression of cardiac and renal dysfunction after 6 weeks AGEs injections. In this study, animals were investigated in compensated hypertrophic phase. We consider this as a primary finding regarding gender differences in cardiac and renal function upon AGE-BSA injections. In the future, the experimental protocol should be optimized with (1) increased AGEs concentration, (2) prolonged injection time, (3) added biomarkers, such as NT-pro-BNP and NGAL, (4) measurement of cytokines, such as TGF-β, involved in fibrosis, and (5) increased sample size in all groups. This study was not designed to investigate the role of sex hormones in AGEs-induced effects on cardiac and renal function. In the future, gender-differences should be investigated by measuring specific estrogen receptors involved in RAGE expression. Using ovariectomized rats would provide further information on gender-related effects of AGEs. Therefore, future perspectives involve investigation of different molecular pathways activated by AGEs in both genders.

6 REFERENCES

1. Ronco C, McCullough PA, Anker SD, Anand I, Aspromonte N, Bagshaw SM, et al. Cardiorenal syndromes: an executive summary from the consensus conference of the Acute Dialysis Quality Initiative (ADQI). Contributions to nephrology. 2010;165:54-67.
2. Damman K, van Deursen VM, Navis G, Voors AA, van Veldhuisen DJ, Hillege HL. Increased central venous pressure is associated with impaired renal function and mortality in a broad spectrum of patients with cardiovascular disease. Journal of the American College of Cardiology. 2009;53(7):582-8.
3. Tang WH, Mullens W. Cardiorenal syndrome in decompensated heart failure. Heart. 2010;96(4):255-60.
4. Kreher P, Ristori MT, Corman B, Verdetti J. Effects of chronic angiotensin I-converting enzyme inhibition on the relations between ventricular action potential changes and myocardial hypertrophy in aging rats. Journal of cardiovascular pharmacology. 1995;25(1):75-80.
5. Schunkert H, Dzau VJ, Tang SS, Hirsch AT, Apstein CS, Lorell BH. Increased rat cardiac angiotensin converting enzyme activity and mRNA expression in pressure overload left ventricular hypertrophy. Effects on coronary resistance, contractility, and relaxation. The Journal of clinical investigation. 1990;86(6):1913-20.
6. Weisman HF, Bush DE, Mannisi JA, Bulkley BH. Global cardiac remodeling after acute myocardial infarction: a study in the rat model. Journal of the American College of Cardiology. 1985;5(6):1355-62.
7. Douglas PS, Katz SE, Weinberg EO, Chen MH, Bishop SP, Lorell BH. Hypertrophic remodeling: gender differences in the early response to left ventricular pressure overload. Journal of the American College of Cardiology. 1998;32(4):1118-25.
8. Leaf DA. Women and coronary artery disease. Gender confers no immunity. Postgraduate medicine. 1990;87(7):55-60.
9. Kannel WB, Schatzkin A. Sudden death: lessons from subsets in population studies. Journal of the American College of Cardiology. 1985;5(6 Suppl):141B-9B.
10. Gordon T, Kannel WB, Hjortland MC, McNamara PM. Menopause and coronary heart disease. The Framingham Study. Annals of internal medicine. 1978;89(2):157-61.
11. Cavasin MA, Tao Z, Menon S, Yang XP. Gender differences in cardiac function during early remodeling after acute myocardial infarction in mice. Life sciences. 2004;75(18):2181-92.
12. Stenvinkel P, Wanner C, Metzger T, Heimburger O, Mallamaci F, Tripepi G, et al. Inflammation and outcome in end-stage renal failure: does female gender constitute a survival advantage? Kidney international. 2002;62(5):1791-8.
13. Wang X, Desai K, Juurlink BH, de Champlain J, Wu L. Gender-related differences in advanced glycation endproducts, oxidative stress markers and nitric oxide synthases in rats. Kidney international. 2006;69(2):281-7.
14. Takahashi M, Suzuki M, Kushida K, Miyamoto S, Inoue T. Relationship between pentosidine levels in serum and urine and activity in rheumatoid arthritis. British journal of rheumatology. 1997;36(6):637-42.
15. Hoshino H, Takahashi M, Kushida K, Ohishi T, Kawana K, Inoue T. Quantitation of the crosslinks, pyridinoline, deoxypyridinoline and pentosidine, in human aorta with dystrophic calcification. Atherosclerosis. 1995;112(1):39-46.
16. Santana RB, Xu L, Chase HB, Amar S, Graves DT, Trackman PC. A role for advanced glycation end products in diminished bone healing in type 1 diabetes. Diabetes. 2003;52(6):1502-10.
17. Thorpe SR, Baynes JW. Maillard reaction products in tissue proteins: new products and new perspectives. Amino acids. 2003;25(3-4):275-81.
18. Hegab Z, Gibbons S, Neyses L, Mamas MA. Role of advanced glycation end products in cardiovascular disease. World journal of cardiology. 2012;4(4):90-102.

19. Hartog JW, Voors AA, Bakker SJ, Smit AJ, van Veldhuisen DJ. Advanced glycation end-products (AGEs) and heart failure: pathophysiology and clinical implications. European journal of heart failure. 2007;9(12):1146-55.
20. Dyer DG, Blackledge JA, Katz BM, Hull CJ, Adkisson HD, Thorpe SR, et al. The Maillard reaction in vivo. Zeitschrift fur Ernahrungswissenschaft. 1991;30(1):29-45.
21. Grandhee SK, Monnier VM. Mechanism of formation of the Maillard protein cross-link pentosidine. Glucose, fructose, and ascorbate as pentosidine precursors. The Journal of biological chemistry. 1991;266(18):11649-53.
22. Koyama Y, Takeishi Y, Arimoto T, Niizeki T, Shishido T, Takahashi H, et al. High serum level of pentosidine, an advanced glycation end product (AGE), is a risk factor of patients with heart failure. Journal of cardiac failure. 2007;13(3):199-206.
23. Schafer S, Huber J, Wihler C, Rutten H, Busch AE, Linz W. Impaired left ventricular relaxation in type 2 diabetic rats is related to myocardial accumulation of N(epsilon)-(carboxymethyl) lysine. European journal of heart failure. 2006;8(1):2-6.
24. Hartog JW, Voors AA, Schalkwijk CG, Scheijen J, Smilde TD, Damman K, et al. Clinical and prognostic value of advanced glycation end-products in chronic heart failure. European heart journal. 2007;28(23):2879-85.
25. Striker LJ, Striker GE. Administration of AGEs in vivo induces extracellular matrix gene expression. Nephrology, dialysis, transplantation : official publication of the European Dialysis and Transplant Association - European Renal Association. 1996;11 Suppl 5:62-5.
26. Huttunen HJ, Fages C, Rauvala H. Receptor for advanced glycation end products (RAGE)-mediated neurite outgrowth and activation of NF-kappaB require the cytoplasmic domain of the receptor but different downstream signaling pathways. The Journal of biological chemistry. 1999;274(28):19919-24.
27. Neumann A, Schinzel R, Palm D, Riederer P, Munch G. High molecular weight hyaluronic acid inhibits advanced glycation endproduct-induced NF-kappaB activation and cytokine expression. FEBS letters. 1999;453(3):283-7.
28. Basta G, Schmidt AM, De Caterina R. Advanced glycation end products and vascular inflammation: implications for accelerated atherosclerosis in diabetes. Cardiovascular research. 2004;63(4):582-92.
29. Ruderman NB, Williamson JR, Brownlee M. Glucose and diabetic vascular disease. FASEB journal : official publication of the Federation of American Societies for Experimental Biology. 1992;6(11):2905-14.
30. Schmidt AM, Yan SD, Stern DM. The dark side of glucose. Nature medicine. 1995;1(10):1002-4.
31. Aronson D. Cross-linking of glycated collagen in the pathogenesis of arterial and myocardial stiffening of aging and diabetes. Journal of hypertension. 2003;21(1):3-12.
32. Zieman S, Kass D. Advanced glycation end product cross-linking: pathophysiologic role and therapeutic target in cardiovascular disease. Congest Heart Fail. 2004;10(3):144-9; quiz 50-1.
33. Stenvinkel P, Alvestrand A. Inflammation in end-stage renal disease: sources, consequences, and therapy. Seminars in dialysis. 2002;15(5):329-37.
34. Neeper M, Schmidt AM, Brett J, Yan SD, Wang F, Pan YC, et al. Cloning and expression of a cell surface receptor for advanced glycosylation end products of proteins. The Journal of biological chemistry. 1992;267(21):14998-5004.
35. Matsumoto S, Yoshida T, Murata H, Harada S, Fujita N, Nakamura S, et al. Solution structure of the variable-type domain of the receptor for advanced glycation end products: new insight into AGE-RAGE interaction. Biochemistry. 2008;47(47):12299-311.
36. Leclerc E, Fritz G, Weibel M, Heizmann CW, Galichet A. S100B and S100A6 differentially modulate cell survival by interacting with distinct RAGE (receptor for advanced glycation end products) immunoglobulin domains. The Journal of biological chemistry. 2007;282(43):31317-31.
37. Colhoun HM, Betteridge DJ, Durrington P, Hitman G, Neil A, Livingstone S, et al. Total soluble and endogenous secretory receptor for advanced glycation end products as predictive biomarkers of

coronary heart disease risk in patients with type 2 diabetes: an analysis from the CARDS trial. Diabetes. 2011;60(9):2379-85.
38. Raposeiras-Roubin S, Rodino-Janeiro BK, Grigorian-Shamagian L, Moure-Gonzalez M, Seoane-Blanco A, Varela-Roman A, et al. Soluble receptor of advanced glycation end products levels are related to ischaemic aetiology and extent of coronary disease in chronic heart failure patients, independent of advanced glycation end products levels: New Roles for Soluble RAGE. European journal of heart failure. 2010;12(10):1092-100.
39. Brett J, Schmidt AM, Yan SD, Zou YS, Weidman E, Pinsky D, et al. Survey of the distribution of a newly characterized receptor for advanced glycation end products in tissues. The American journal of pathology. 1993;143(6):1699-712.
40. Boulanger E, Wautier MP, Wautier JL, Boval B, Panis Y, Wernert N, et al. AGEs bind to mesothelial cells via RAGE and stimulate VCAM-1 expression. Kidney international. 2002;61(1):148-56.
41. Sun M, Yokoyama M, Ishiwata T, Asano G. Deposition of advanced glycation end products (AGE) and expression of the receptor for AGE in cardiovascular tissue of the diabetic rat. International journal of experimental pathology. 1998;79(4):207-22.
42. He CJ, Zheng F, Stitt A, Striker L, Hattori M, Vlassara H. Differential expression of renal AGE-receptor genes in NOD mice: possible role in nonobese diabetic renal disease. Kidney international. 2000;58(5):1931-40.
43. Raucci A, Cugusi S, Antonelli A, Barabino SM, Monti L, Bierhaus A, et al. A soluble form of the receptor for advanced glycation endproducts (RAGE) is produced by proteolytic cleavage of the membrane-bound form by the sheddase a disintegrin and metalloprotease 10 (ADAM10). FASEB journal : official publication of the Federation of American Societies for Experimental Biology. 2008;22(10):3716-27.
44. Kalea AZ, Schmidt AM, Hudson BI. RAGE: a novel biological and genetic marker for vascular disease. Clin Sci (Lond). 2009;116(8):621-37.
45. Kislinger T, Fu C, Huber B, Qu W, Taguchi A, Du Yan S, et al. N(epsilon)-(carboxymethyl)lysine adducts of proteins are ligands for receptor for advanced glycation end products that activate cell signaling pathways and modulate gene expression. The Journal of biological chemistry. 1999;274(44):31740-9.
46. Wautier MP, Chappey O, Corda S, Stern DM, Schmidt AM, Wautier JL. Activation of NADPH oxidase by AGE links oxidant stress to altered gene expression via RAGE. American journal of physiology Endocrinology and metabolism. 2001;280(5):E685-94.
47. Yan SF, Ramasamy R, Schmidt AM. The RAGE axis: a fundamental mechanism signaling danger to the vulnerable vasculature. Circulation research. 2010;106(5):842-53.
48. Bucciarelli LG, Wendt T, Qu W, Lu Y, Lalla E, Rong LL, et al. RAGE blockade stabilizes established atherosclerosis in diabetic apolipoprotein E-null mice. Circulation. 2002;106(22):2827-35.
49. Falcone C, Emanuele E, D'Angelo A, Buzzi MP, Belvito C, Cuccia M, et al. Plasma levels of soluble receptor for advanced glycation end products and coronary artery disease in nondiabetic men. Arteriosclerosis, thrombosis, and vascular biology. 2005;25(5):1032-7.
50. Kalousova M, Hodkova M, Kazderova M, Fialova J, Tesar V, Dusilova-Sulkova S, et al. Soluble receptor for advanced glycation end products in patients with decreased renal function. American journal of kidney diseases : the official journal of the National Kidney Foundation. 2006;47(3):406-11.
51. Beisswenger PJ, Howell S, Mackenzie T, Corstjens H, Muizzuddin N, Matsui MS. Two fluorescent wavelengths, 440(ex)/520(em) nm and 370(ex)/440(em) nm, reflect advanced glycation and oxidation end products in human skin without diabetes. Diabetes technology & therapeutics. 2012;14(3):285-92.
52. Zhang FL, Gao HQ, Shen L. Inhibitory effect of GSPE on RAGE expression induced by advanced glycation end products in endothelial cells. Journal of cardiovascular pharmacology. 2007;50(4):434-40.

53. Skavdahl M, Steenbergen C, Clark J, Myers P, Demianenko T, Mao L, et al. Estrogen receptor-beta mediates male-female differences in the development of pressure overload hypertrophy. American journal of physiology Heart and circulatory physiology. 2005;288(2):H469-76.
54. van Eickels M, Grohe C, Cleutjens JP, Janssen BJ, Wellens HJ, Doevendans PA. 17beta-estradiol attenuates the development of pressure-overload hypertrophy. Circulation. 2001;104(12):1419-23.
55. Baynes J, Murray DB. Cardiac and renal function are progressively impaired with aging in Zucker diabetic fatty type II diabetic rats. Oxidative medicine and cellular longevity. 2009;2(5):328-34.
56. Herrmann KL, McCulloch AD, Omens JH. Glycated collagen cross-linking alters cardiac mechanics in volume-overload hypertrophy. American journal of physiology Heart and circulatory physiology. 2003;284(4):H1277-84.
57. Umadevi S, Gopi V, Elangovan V. Regulatory mechanism of gallic acid against advanced glycation end products induced cardiac remodeling in experimental rats. Chemico-biological interactions. 2014;208:28-36.
58. Sanderson JE, Lai KB, Shum IO, Wei S, Chow LT. Transforming growth factor-beta(1) expression in dilated cardiomyopathy. Heart. 2001;86(6):701-8.
59. Mukherjee TK, Reynolds PR, Hoidal JR. Differential effect of estrogen receptor alpha and beta agonists on the receptor for advanced glycation end product expression in human microvascular endothelial cells. Biochimica et biophysica acta. 2005;1745(3):300-9.
60. Lu L, Zhang Q, Xu Y, Zhu ZB, Geng L, Wang LJ, et al. Intra-coronary administration of soluble receptor for advanced glycation end-products attenuates cardiac remodeling with decreased myocardial transforming growth factor-beta1 expression and fibrosis in minipigs with ischemia-reperfusion injury. Chinese medical journal. 2010;123(5):594-8.
61. Nerlich AG, Schleicher ED. N(epsilon)-(carboxymethyl)lysine in atherosclerotic vascular lesions as a marker for local oxidative stress. Atherosclerosis. 1999;144(1):41-7.
62. Lieuw AFML, van Hinsbergh VW, Teerlink T, Barto R, Twisk J, Stehouwer CD, et al. Increased levels of N(epsilon)-(carboxymethyl)lysine and N(epsilon)-(carboxyethyl)lysine in type 1 diabetic patients with impaired renal function: correlation with markers of endothelial dysfunction. Nephrology, dialysis, transplantation : official publication of the European Dialysis and Transplant Association - European Renal Association. 2004;19(3):631-6.
63. Gugliucci A, Bendayan M. Renal fate of circulating advanced glycated end products (AGE): evidence for reabsorption and catabolism of AGE-peptides by renal proximal tubular cells. Diabetologia. 1996;39(2):149-60.
64. Peleg I, Greenfeld Z, Cooperman H, Shoshan S. Type I and type III collagen mRNA levels in kidney regions of old and young rats. Matrix. 1993;13(4):281-7.
65. Coughlan MT, Yap FY, Tong DC, Andrikopoulos S, Gasser A, Thallas-Bonke V, et al. Advanced glycation end products are direct modulators of beta-cell function. Diabetes. 2011;60(10):2523-32.

SUPPLEMENTAL DATA

S1

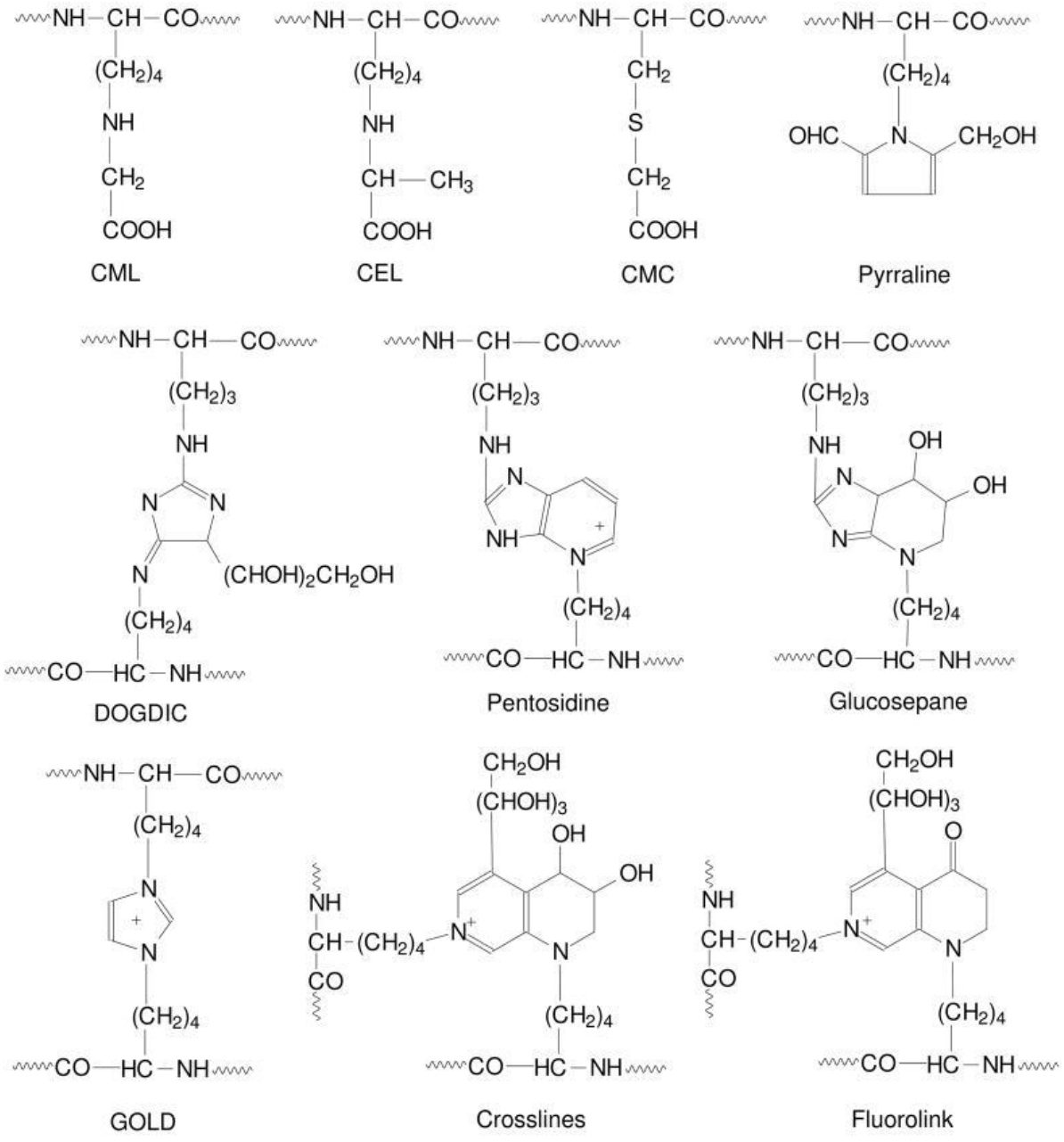

Figure S1: Chemical structure of the AGE isoforms.
AGEs include *Nε*-(carboxymethyl)lysine (CML), *Nε*-(carboxylethyllysine) (CEL), *S*-(carboxymethyl)cysteine (CMC), pyrraline, 3-deoxyglucosone-derived imidazolium crosslink (DOGDIC), pentosidine, glucosepane, glyoxal lysine dimer (GOLD), crosslines, and fluorolink. Three main groups of AGEs have been described: (1) fluorescent cross-linking AGEs; (2) non-fluorescent cross-linking AGEs; (3) non-cross-linking AGEs. Zhang *et al.*2010.

Auteursrechtelijke overeenkomst

Ik/wij verlenen het wereldwijde auteursrecht voor de ingediende eindverhandeling:
Gender-related effects of advanced glycation end products on cardiac and renal function

Richting: **master in de biomedische wetenschappen-klinische moleculaire wetenschappen**
Jaar: **2014**

in alle mogelijke mediaformaten, - bestaande en in de toekomst te ontwikkelen - , aan de Universiteit Hasselt.

Niet tegenstaand deze toekenning van het auteursrecht aan de Universiteit Hasselt behoud ik als auteur het recht om de eindverhandeling, - in zijn geheel of gedeeltelijk -, vrij te reproduceren, (her)publiceren of distribueren zonder de toelating te moeten verkrijgen van de Universiteit Hasselt.

Ik bevestig dat de eindverhandeling mijn origineel werk is, en dat ik het recht heb om de rechten te verlenen die in deze overeenkomst worden beschreven. Ik verklaar tevens dat de eindverhandeling, naar mijn weten, het auteursrecht van anderen niet overtreedt.

Ik verklaar tevens dat ik voor het materiaal in de eindverhandeling dat beschermd wordt door het auteursrecht, de nodige toelatingen heb verkregen zodat ik deze ook aan de Universiteit Hasselt kan overdragen en dat dit duidelijk in de tekst en inhoud van de eindverhandeling werd genotificeerd.

Universiteit Hasselt zal mij als auteur(s) van de eindverhandeling identificeren en zal geen wijzigingen aanbrengen aan de eindverhandeling, uitgezonderd deze toegelaten door deze overeenkomst.

Voor akkoord,

Arslan, Tugçe

Datum: **19/08/2014**